

# Mitochondrial respiratory states and rates

**COST Action CA15203 MitoEAGLE preprint** Version: 2018-12-01 (49)

Corresponding author: Gnaiger E

Authors:

Gnaiger E, Aasander Frostner E, Abumrad NA, Acuna-Castroviejo D, Adiele RC, Ahn B, Ali SS, Alton L, Alves MG, Amati F, Amoedo ND, Andreadou I, Aragón M, Aral C, Arandarčikaitė O, Armand AS, Arnould T, Avram VF, Bailey DM, Bajpeyi S, Bajzikova M, Bakker BM, Bastos Sant'Anna Silva AC, Batterson P, Battino M, Bazil J, Beard DA, Bednarczyk P, Bello F, Ben-Shachar D, Bergdahl A, Berge RK, Bergmeister L, Bernardi P, Berridge MV, Bettinazzi S, Bishop D, Blier PU, Blindheim DF, Boardman NT, Boetker HE, Borchard S, Boros M, Børsheim E, Borutaite V, Botella Ruiz J, Bouillaud F, Bouitbir J, Boushel RC, Bovard J, Breton S, Brown DA, Brown GC, Brown RA, Brozinick JT, Buettner GR, Burtscher J, Calabria E, Calbet JA, Calzia E, Cannon DT, Cano Sanchez M, Canto AC, Cardoso LHD, Carvalho E, Casado Pinna M, Cassar S, Cassina AM, Castelo MP, Castro L, Cavalcanti-de-Albuquerque JP, Cervinkova Z, Chabi B, Chakrabarti L, Chakrabarti S, Chaurasia B, Chen Q, Chicco AJ, Chinopoulos C, Chowdhury SK, Cizmarova B, Clementi E, Coen PM, Cohen BH, Coker RH, Collin A, Crisóstomo L, Dahdah N, Dambrova M, Danhelovska T, Darveau CA, Das AM, Dash RK, Davidova E, Davis MS, De Goede P, De Palma C, Dembinska-Kiec A, Detraux D, Devaux Y, Di Marcello M, Dias TR, Distefano G, Doermann N, Doerrier C, Dong L, Donnelly C, Drahota Z, Duarte FV, Dubouchaud H, Duchon MR, Dumas JF, Durham WJ, Dymkowska D, Dyrstad SE, Dyson A, Dzialowski EM, Eaton S, Ehinger J, Elmer E, Endlicher R, Engin AB, Escames G, Ezrova Z, Falk MJ, Fell DA, Ferdinandy P, Ferko M, Ferreira JCB, Ferreira R, Ferri A, Fessel JP, Filipovska A, Fisar Z, Fischer C, Fischer M, Fisher G, Fisher JJ, Ford E, Fornaro M, Galina A, Galkin A, Galli GL, Gan Z, Ganetzky R, Garcia-Roves PM, Garcia-Souza LF, Garipi E, Garlid KD, Garrabou G, Garten A, Gastaldelli A, Gayen J, Genders A, Genova ML, Giovarelli M, Gonzalez-Armenta JL, Goncalo Teixeira da SR, Gonzalo H, Goodpaster BH, Gorr TA, Gourlay CW, Granata C, Grefte S, Guarch ME, Gueguen N, Gumeni S, Haas CB, Haavik J, Haendeler J, Hamann A, Han J, Han WH, Hancock CR, Hand SC, Handl J, Hargreaves IP, Harper ME, Harrison DK, Hausenloy DJ, Heales SJR, Heiestad C, Hellgren KT, Hepple RT, Hernansanz-Agustin P, Hewakapuge S, Hickey AJ, Hoehn KL, Hoel F, Holland OJ, Holloway GP, Hoppel CL, Hoppel F, Houstek J, Huete-Ortega M, Hyrossova P, Iglesias-Gonzalez J, Irving BA, Isola R, Iyer S, Jackson CB, Jadiya P, Jana PF, Jang DH, Jang YC, Janowska J, Jansen K, Jansen-Dürr P, Jansone B, Jarmuszkiewicz W, Jaskiewicz A, Jespersen NR, Jha RK, Jurczak MJ, Jurk D, Kaambre T, Kaczor JJ, Kainulainen H, Kampa RP, Kandel SM, Kane DA, Kang Y, Kappler L, Karabatsiakos A, Karkucinska-Wieckowska A, Kaur S, Keijer J, Keller MA, Keppner G, Khamoui AV, Kidere D, Kilbaugh T, Kim HK, Kim JKS, Klepinin A, Klingenspor M, Komlodi T, Koopman WJH, Kopitar-Jerala N, Kowaltowski AJ, Kozlov AV, Krajcova A, Krako Jakovljevic N, Kristal BS, Krumschnabel G, Krycer JR, Kuang J, Kucera O, Kuka J, Kwak HB, Kwast K, Laasmaa M, Labieniec-Watala M, Lai N, Land JM, Lane N, Laner V, Lanza IR, Larsen TS, Lavery GG, Lazou A, Lee HK, Leeuwenburgh C, Lehti M, Lemieux H, Lenaz G, Lerfall J, Li PA, Li Puma L, Liepins E, Lionett S, Liu J, López LC, Lucchinetti E, Ma T, Macedo MP, MacMillan-Crow LA, Majtnerova P, Makarova E, Makrecka-Kuka M, Malik AN, Markova M, Martins AD, Martin DS, Martins JD, Mazat JP, McKenna HT, Menze MA, Merz T, Meszaros AT, Methner A, Michalak S, Moellering DR, Moiso N, Molina AJA, Montaine D, Moore AL, Moreau K, Moreno-Sánchez R, Moreira BP, Mracek T, Muccini AM, Muntane J, Muntean DM, Murray AJ, Musiol E, Myhre Pedersen T, Nair KS, Nehlin JO, Nemeč M,

49 Neufer PD, Neuzil J, Nevriere R, Newsom S, Nozickova K, O'Brien KA, O'Gorman D, Olgar Y, Oliveira  
 50 MF, Oliveira MT, Oliveira PF, Oliveira PJ, Orynbayeva Z, Osiewacz HD, Ounpuu L, Pak YK, Pallotta  
 51 ML, Palmeira CM, Parajuli N, Passos JF, Passrigger M, Patel HH, Pavlova N, Pecina P, Pereira da  
 52 Silva Grilo da Silva F, Perez Valencia JA, Perks K, Pesta D, Petit PX, Pettersen IKN, Pichaud N, Pichler  
 53 I, Piel S, Pietka TA, Pino MF, Pirkmajer S, Porter C, Porter RK, Procaccio V, Prochownik EV,  
 54 Pulinilkunnil T, Puskarich MA, Puurand M, Radenkovic F, Ramzan R, Rattan SIS, Reboredo P, Renner-  
 55 Sattler K, Rial E, Robinson MM, Roden M, Rodríguez-Enriquez S, Rohlena J, Rolo AP, Ropelle ER,  
 56 Røsland GV, Rossignol R, Rossiter HB, Rubelj I, Rybacka-Mossakowska J, Saada A, Safaei Z, Salin  
 57 K, Salvadego D, Sandi C, Saner N, Sanz A, Sazanov LA, Scatena R, Schartner M, Scheibye-Knudsen  
 58 M, Schilling JM, Schlattner U, Schönfeld P, Schots PC, Schulz R, Schwarzer C, Scott GR, Selman C,  
 59 Shabalina IG, Sharma P, Sharma V, Shevchuk I, Siewiera K, Silber AM, Silva AM, Sims CA, Singer  
 60 D, Singh, BK, Skolik R, Smenes BT, Smith J, Soares FAA, Sobotka O, Sokolova I, Sonkar VK, Sowton  
 61 AP, Sparagna GC, Sparks LM, Spinazzi M, Stankova P, Starr J, Stary C, Stelfa G, Stepto NK, Stiban J,  
 62 Stier A, Stocker R, Storder J, Suomalainen A, Sumbalova Z, Suravajhala P, Svalbe B, Swerdlow RH,  
 63 Swiniuch D, Szabo I, Szewczyk A, Szibor M, Tanaka M, Tandler B, Tarnopolsky MA, Tausan D,  
 64 Tavernarakis N, Tepp K, Thakkar H, Thyfault JP, Tomar D, Torp MK, Towheed A, Tretter L, Trifunovic  
 65 A, Trivigno C, Tronstad KJ, Trougakos IP, Truu L, Tuncay E, Turan B, Tyrrell DJ, Urban T, Valentine  
 66 JM, Van Bergen NJ, Van Hove J, Varricchio F, Vella J, Vendelin M, Vercesi AE, Victor VM, Vieira  
 67 Ligo Teixeira C, Vidimce J, Viel C, Vieyra A, Vilks K, Villena JA, Vincent V, Vinogradov AD, Viscomi  
 68 C, Vitorino RMP, Vogt S, Volani C, Volska K, Votion DM, Vujacic-Mirski K, Wagner BA, Ward ML,  
 69 Warnsmann V, Wasserman DH, Watala C, Wei YH, Whitfield J, Wickert A, Wieckowski MR, Wiesner  
 70 RJ, Williams C, Winwood-Smith H, Wohlgemuth SE, Wohlwend M, Wolff JN, Wrutniak-Cabello C,  
 71 Wüst RCI, Yokota T, Zablocki K, Zanon A, Zaugg K, Zaugg M, Zdrzilova L, Zhang Y, Zhang YZ,  
 72 Zíková A, Zischka H, Zorzano A, Zvejniece L

73

74

#### Updates and discussion:

75

[http://www.mitoeagle.org/index.php/MitoEAGLE\\_preprint\\_2018-02-08](http://www.mitoeagle.org/index.php/MitoEAGLE_preprint_2018-02-08)

76

77

501 coauthors

78

79

Correspondence: Gnaiger E

80

*Chair COST Action CA15203 MitoEAGLE – <http://www.mitoeagle.org>*

81

*Department of Visceral, Transplant and Thoracic Surgery, D. Swarovski Research Laboratory,*

82

*Medical University of Innsbruck, Innrain 66/4, A-6020 Innsbruck, Austria*

83

*Email: [mitoeagle@i-med.ac.at](mailto:mitoeagle@i-med.ac.at); Tel: +43 512 566796, Fax: +43 512 566796 20*

84



85	<b>Table of contents</b>
86	
87	<b>Abstract</b>
88	<b>Executive summary</b>
89	<b>1. Introduction</b> – Box 1: In brief: Mitochondria and Bioblasts
90	<b>2. Coupling states and rates in mitochondrial preparations</b>
91	2.1. <i>Cellular and mitochondrial respiration</i>
92	2.1.1. Aerobic and anaerobic catabolism and ATP turnover
93	2.1.2. Specification of biochemical dose
94	2.2. <i>Mitochondrial preparations</i>
95	2.3. <i>Electron transfer pathways</i>
96	2.4. <i>Respiratory coupling control</i>
97	2.4.1. Coupling
98	2.4.2. Phosphorylation, P <sub>o</sub> , and P <sub>o</sub> /O <sub>2</sub> ratio
99	2.4.3. Uncoupling
100	2.5. <i>Coupling states and respiratory rates</i>
101	2.5.1. <b>LEAK-state</b>
102	2.5.2. <b>OXPHOS-state</b>
103	2.5.3. <b>Electron transfer-state</b>
104	2.5.4. ROX state and <i>Rox</i>
105	2.5.5. Quantitative relations
106	2.5.6. The steady-state
107	2.6. <i>Classical terminology for isolated mitochondria</i>
108	2.6.1. State 1
109	2.6.2. State 2
110	2.6.3. State 3
111	2.6.4. State 4
112	2.6.5. State 5
113	2.7. <i>Control and regulation</i>
114	<b>3. What is a rate?</b> – Box 2: Metabolic flows and fluxes: vectorial, vectorial, and scalar
115	<b>4. Normalization of rate per sample</b>
116	4.1. <i>Flow: per object</i>
117	4.1.1. Number concentration
118	4.1.2. Flow per object
119	4.2. <i>Size-specific flux: per sample size</i>
120	4.2.1. Sample concentration
121	4.2.2. Size-specific flux
122	4.3. <i>Marker-specific flux: per mitochondrial content</i>
123	4.3.1. Mitochondrial concentration and mitochondrial markers
124	4.3.2. mt-Marker-specific flux
125	<b>5. Normalization of rate per system</b>
126	5.1. <i>Flow: per chamber</i>
127	5.2. <i>Flux: per chamber volume</i>
128	5.2.1. System-specific flux
129	5.2.2. Advancement per volume
130	<b>6. Conversion of units</b>
131	<b>7. Conclusions</b> – Box 3: Recommendations for studies with mitochondrial preparations
132	<b>References</b>
133	<b>Supplement</b>
134	S1. Manuscript phases and versions - an open-access approach
135	S2. Authors
136	S3. Joining COST Actions
137	

138 **Abstract** As the knowledge base and importance of mitochondrial physiology to human health expands,  
 139 the necessity for harmonizing the terminology concerning mitochondrial respiratory states and rates has  
 140 become increasingly apparent. The chemiosmotic theory establishes the mechanism of energy  
 141 transformation and coupling in oxidative phosphorylation. The unifying concept of the protonmotive  
 142 force provides the framework for developing a consistent theoretical foundation of mitochondrial  
 143 physiology and bioenergetics. We follow IUPAC guidelines on terminology in physical chemistry,  
 144 extended by considerations of open systems and thermodynamics of irreversible processes. The concept-  
 145 driven constructive terminology incorporates the meaning of each quantity and aligns concepts and  
 146 symbols with the nomenclature of classical bioenergetics. We endeavour to provide a balanced view of  
 147 mitochondrial respiratory control and a critical discussion on reporting data of mitochondrial respiration  
 148 in terms of metabolic flows and fluxes. Uniform standards for evaluation of respiratory states and rates  
 149 will ultimately contribute to reproducibility between laboratories and thus support the development of  
 150 databases of mitochondrial respiratory function in species, tissues, and cells. Clarity of concept and  
 151 consistency of nomenclature facilitate effective transdisciplinary communication, education, and  
 152 ultimately further discovery.

153  
 154 *Keywords:* Mitochondrial respiratory control, coupling control, mitochondrial preparations,  
 155 protonmotive force, uncoupling, oxidative phosphorylation: OXPHOS, efficiency, electron transfer: ET,  
 156 electron transfer system: ETS, proton leak, ion leak and slip compensatory state: LEAK, residual oxygen  
 157 consumption: ROX, State 2, State 3, State 4, normalization, flow, flux, oxygen: O<sub>2</sub>  
 158

---

## 159 **Executive summary**

160  
 161 In view of the broad implications for health care, mitochondrial researchers face an increasing  
 162 responsibility to disseminate their fundamental knowledge and novel discoveries to a wide range of  
 163 stakeholders and scientists beyond the group of specialists. This requires implementation of a commonly  
 164 accepted terminology within the discipline and standardization in the translational context. Authors,  
 165 reviewers, journal editors, and lecturers are challenged to collaborate with the aim to harmonize the  
 166 nomenclature in the growing field of mitochondrial physiology and bioenergetics, from evolutionary  
 167 biology and comparative physiology to mitochondrial medicine. In the present communication we focus  
 168 on the following concepts in mitochondrial physiology:

- 169 1. Aerobic respiration depends on the coupling of phosphorylation (ADP → ATP) to O<sub>2</sub> flux in  
 170 catabolic reactions. Coupling in oxidative phosphorylation is mediated by the translocation of  
 171 protons across the mitochondrial inner membrane (mtIM) through proton pumps generating  
 172 or utilizing the protonmotive force that is maintained between the mitochondrial matrix and  
 173 intermembrane compartment or outer mitochondrial space. Compartmental coupling  
 174 distinguishes this vectorial component of oxidative phosphorylation from glycolytic  
 175 fermentation as the counterpart of cellular core energy metabolism (**Figure 1**). Cell respiration  
 176 is distinguished from fermentation: (1) Electron acceptors are supplied by external respiration  
 177 for the maintenance of redox balance, whereas fermentation is characterized by an internal  
 178 electron acceptor produced in intermediary metabolism. In aerobic cell respiration, redox  
 179 balance is maintained by O<sub>2</sub> as the electron acceptor. (2) Compartmental coupling in vectorial  
 180 oxidative phosphorylation contrasts to exclusively scalar substrate-level phosphorylation in  
 181 fermentation.
- 182 2. When measuring mitochondrial metabolism, the contribution of fermentation and other cytosolic  
 183 interactions must be excluded from analysis by disrupting the barrier function of the plasma  
 184 membrane. Selective removal or permeabilization of the plasma membrane yields  
 185 mitochondrial preparations—including isolated mitochondria, tissue and cellular  
 186 preparations—with structural and functional integrity. Subsequently, extra-mitochondrial  
 187 concentrations of fuel substrates, ADP, ATP, inorganic phosphate, and cations including H<sup>+</sup>  
 188 can be controlled to determine mitochondrial function under a set of conditions defined as  
 189 coupling control states. We strive to incorporate an easily recognized and understood concept-  
 190 driven terminology of bioenergetics with explicit terms and symbols that define the nature of  
 191 respiratory states.
- 192 3. Mitochondrial coupling states are defined according to the control of respiratory oxygen flux by  
 193 the protonmotive force. Capacities of oxidative phosphorylation and electron transfer are



measured at kinetically saturating concentrations of fuel substrates, ADP and inorganic phosphate, and O<sub>2</sub>, or at optimal uncoupler concentrations, respectively, in the absence of Complex IV inhibitors such as NO, CO, or H<sub>2</sub>S. Respiratory capacity is a measure of the upper boundary of the rate of respiration; it depends on the substrate type undergoing oxidation, and provides reference values for the diagnosis of health and disease, and for evaluation of the effects of Evolutionary background, Age, Gender and sex, Lifestyle and Environment.

### Figure 1. Internal and external respiration

Mitochondrial respiration is the oxidation of fuel substrates (electron donors) and reduction of O<sub>2</sub> catalysed by the electron transfer system, ETS: (mt) mitochondrial catabolic respiration; (ce) total cellular O<sub>2</sub> consumption; and (ext) external respiration. All chemical reactions,  $r$ , that consume O<sub>2</sub> in the cells of an organism, contribute to cell respiration,  $J_{rO_2}$ . In addition to mitochondrial catabolic respiration, O<sub>2</sub> is consumed by:

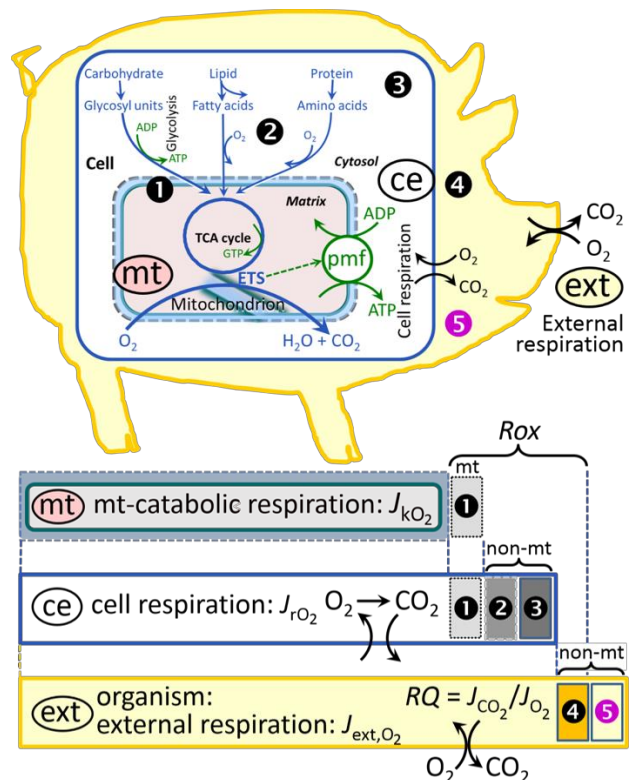
① Mitochondrial residual O<sub>2</sub> consumption,  $Rox$ .  
 ② Non-mitochondrial O<sub>2</sub> consumption by catabolic reactions, particularly peroxisomal oxidases and microsomal cytochrome P450 systems. ③ Non-mitochondrial  $Rox$  by reactions unrelated to catabolism. ④ Extracellular  $Rox$ . ⑤ Aerobic microbial respiration. Bars are not at a quantitative scale.

(mt) **Mitochondrial catabolic respiration**,  $J_{kO_2}$ , is the O<sub>2</sub> consumption by the mitochondrial ETS excluding  $Rox$ .

(ce) **Cell respiration**,  $J_{rO_2}$ , takes into account

internal O<sub>2</sub>-consuming reactions,  $r$ , including catabolic respiration and  $Rox$ . Catabolic cell respiration is the O<sub>2</sub> consumption associated with catabolic pathways in the cell, including mitochondrial catabolism in addition to peroxisomal and microsomal oxidation reactions (②).

(ext) **External respiration** balances internal respiration at steady-state, including extracellular  $Rox$  (④) and aerobic respiration by the microbiome (⑤). O<sub>2</sub> is transported from the environment across the respiratory cascade, *i.e.*, circulation between tissues and diffusion across cell membranes, to the intracellular compartment. The respiratory quotient,  $RQ$ , is the molar CO<sub>2</sub>/O<sub>2</sub> exchange ratio; when combined with the respiratory nitrogen quotient, N/O<sub>2</sub> (mol N given off per mol O<sub>2</sub> consumed), the  $RQ$  reflects the proportion of carbohydrate, lipid and protein utilized in cell respiration during aerobically balanced steady-states. Bicarbonate and CO<sub>2</sub> are transported in reverse to the extracellular milieu and the organismic environment. Hemoglobin provides the molecular paradigm for the combination of O<sub>2</sub> and CO<sub>2</sub> exchange, as do lungs and gills on the morphological level.



4. Incomplete tightness of coupling, *i.e.*, some degree of uncoupling relative to the substrate-dependent coupling stoichiometry, is a characteristic of energy-transformations across membranes. Uncoupling is caused by a variety of physiological, pathological, toxicological, pharmacological and environmental conditions that exert an influence not only on the proton leak and cation cycling, but also on proton slip within the proton pumps and the structural integrity of the mitochondria. A more loosely coupled state is induced by stimulation of mitochondrial superoxide formation and the bypass of proton pumps. In addition, the use of protonophores represents an experimental uncoupling intervention to assess the transition from a well-coupled to a noncoupled state of mitochondrial respiration.

5. Respiratory oxygen consumption rates have to be carefully normalized to enable meta-analytic studies beyond the question of a particular experiment. Therefore, all raw data on rates and variables for normalization should be published in an open access data repository. Normalization of rates for: (1) the number of objects (cells, organisms); (2) the volume or

250 mass of the experimental sample; and (3) the concentration of mitochondrial markers in the  
 251 experimental chamber are sample-specific normalizations, which are distinguished from  
 252 system-specific normalization for the volume of the chamber (the measuring system).  
 253 6. The consistent use of terms and symbols will facilitate transdisciplinary communication and  
 254 support the further development of a collaborative database on bioenergetics and  
 255 mitochondrial physiology. The present considerations are focused on studies with  
 256 mitochondrial preparations. These will be extended in a series of reports on pathway control  
 257 of mitochondrial respiration, respiratory states in intact cells, and harmonization of  
 258 experimental procedures.  
 259

---

### 260 **Box 1: In brief – Mitochondria and Bioblasts**

261 *‘For the physiologist, mitochondria afforded the first opportunity for an experimental*  
 262 *approach to structure-function relationships, in particular those involved in active*  
 263 *transport, vectorial metabolism, and metabolic control mechanisms on a subcellular level’*  
 264 *(Ernster and Schatz 1981).*

265 Mitochondria are oxygen-consuming electrochemical generators that evolved from the endosymbiotic  
 266 alphaproteobacteria which became integrated into a host cell related to Asgard Archaea (Margulis 1970;  
 267 Lane 2005; Roger *et al.* 2017). They were described by Richard Altmann (1894) as ‘bioblasts’, which  
 268 include not only the mitochondria as presently defined, but also symbiotic and free-living bacteria. The  
 269 word ‘mitochondria’ (Greek mitos: thread; chondros: granule) was introduced by Carl Benda (1898).

270 Contrary to current textbook dogma, mitochondria form dynamic networks within eukaryotic  
 271 cells. Mitochondrial movement is supported by microtubules and morphology can change in response  
 272 to energy requirements of the cell via processes known as fusion and fission; these interactions allow  
 273 mitochondria to communicate within a network (Chan 2006). Mitochondria can even traverse cell  
 274 boundaries in a process known as horizontal mitochondrial transfer (Torralba *et al.* 2016). Another  
 275 defining characteristic of mitochondria is the double membrane. The mitochondrial inner membrane  
 276 (mtIM) forms dynamic tubular to disk-shaped cristae that separate the mitochondrial matrix, *i.e.*, the  
 277 negatively charged internal mitochondrial compartment, from the intermembrane space; the latter being  
 278 enclosed by the mitochondrial outer membrane (mtOM) and positively charged with respect to the  
 279 matrix. The mtIM contains the non-bilayer phospholipid cardiolipin, which is not present in any other  
 280 eukaryotic cellular membrane. Cardiolipin has many regulatory functions (Oemer *et al.* 2018); in  
 281 particular, it stabilizes and promotes the formation of respiratory supercomplexes (SC I<sub>n</sub>III<sub>n</sub>IV<sub>n</sub>), which  
 282 are supramolecular assemblies based upon specific and dynamic interactions between individual  
 283 respiratory complexes (Greggio *et al.* 2017; Lenaz *et al.* 2017). The mitochondrial membrane is plastic  
 284 and exerts an influence on the functional properties of proteins incorporated in membranes  
 285 (Waczulikova *et al.* 2007). Intracellular stress factors may cause shrinking or swelling of the  
 286 mitochondrial matrix that can ultimately result in permeability transition.

287 Mitochondria are the structural and functional elementary components of cell respiration.  
 288 Mitochondrial respiration is the reduction of molecular oxygen by electron transfer coupled to  
 289 electrochemical proton translocation across the mtIM. In the process of oxidative phosphorylation  
 290 (OXPHOS), the catabolic reaction of oxygen consumption is electrochemically coupled to the  
 291 transformation of energy in the form of adenosine triphosphate (ATP; Mitchell 1961, 2011).  
 292 Mitochondria are the powerhouses of the cell that contain the machinery of the OXPHOS-pathways,  
 293 including transmembrane respiratory complexes (proton pumps with FMN, Fe-S and cytochrome *b*, *c*,  
 294 *aa*<sub>3</sub> redox systems); alternative dehydrogenases and oxidases; the coenzyme ubiquinone (Q); F-ATPase  
 295 or ATP synthase; the enzymes of the tricarboxylic acid cycle (TCA), fatty acid and amino acid oxidation;  
 296 transporters of ions, metabolites and co-factors; iron/sulphur cluster synthesis; and mitochondrial  
 297 kinases related to catabolic pathways. The mitochondrial proteome comprises over 1,200 proteins  
 298 (Calvo *et al.* 2015; 2017), mostly encoded by nuclear DNA (nDNA), with a variety of functions, many  
 299 of which are relatively well known, *e.g.*, proteins regulating mitochondrial biogenesis or apoptosis,  
 300 while others are still under investigation, or need to be identified, *e.g.*, permeability transition pore,  
 301 alanine transporter. Only recently has it been possible to use the mammalian mitochondrial proteome to  
 302 discover and characterize the genetic basis of mitochondrial diseases (Williams *et al.* 2016; Palmfeldt  
 303 and Bross 2017).

304 Numerous cellular processes are orchestrated by a constant crosstalk between mitochondria and  
 305 other cellular components. For example, the crosstalk between mitochondria and the endoplasmic

306 reticulum is involved in the regulation of calcium homeostasis, cell division, autophagy, differentiation,  
 307 and anti-viral signaling (Murley and Nunnari 2016). Mitochondria contribute to the formation of  
 308 peroxisomes, which are hybrids of mitochondrial and ER-derived precursors (Sugiura *et al.* 2017).  
 309 Cellular mitochondrial homeostasis (mitostasis) is maintained through regulation at transcriptional,  
 310 post-translational and epigenetic levels. Cell signalling modules contribute to homeostatic regulation  
 311 throughout the cell cycle or even cell death by activating proteostatic modules, *e.g.*, the ubiquitin-  
 312 proteasome and autophagy-lysosome/vacuole pathways; specific proteases like LON, and genome  
 313 stability modules in response to varying energy demands and stress cues (Quiros *et al.* 2016). Several  
 314 post-translational modifications, including acetylation and nitrosylation, are also capable of influencing  
 315 the bioenergetic response, with clinically significant implications for health and disease (Carrico *et al.*  
 316 2018).

317 Mitochondria of higher eukaryotes typically maintain several copies of their own circular genome  
 318 known as mitochondrial DNA (mtDNA; hundred to thousands per cell; Cummins 1998), which is  
 319 maternally inherited in humans. Biparental mitochondrial inheritance is documented in mammals, birds,  
 320 fish, reptiles and invertebrate groups, and is even the norm in some bivalve taxonomic groups (Breton  
 321 *et al.* 2007; White *et al.* 2008). The mitochondrial genome of the angiosperm *Amborella* contains a  
 322 record of six mitochondrial genome equivalents acquired by horizontal transfer of entire genomes, two  
 323 from angiosperms, three from algae and one from mosses (Rice *et al.* 2016). In unicellular organisms,  
 324 *i.e.*, protists, the structural organization of mitochondrial genomes is highly variable and includes  
 325 circular and linear DNA (Zikova *et al.* 2016). While some of the free-living flagellates exhibit the largest  
 326 known gene coding capacity, *e.g.*, jakobid *Andalucia godoyi* mitochondrial DNA codes for 106 genes  
 327 (Burger *et al.* 2013), some protist groups, *e.g.*, alveolates, possess mitochondrial genomes with only  
 328 three protein-coding genes and two rRNAs (Feagin *et al.* 2012). The complete loss of mitochondrial  
 329 genome is observed in highly reduced mitochondria of *Cryptosporidium* species (Liu *et al.* 2016).  
 330 Reaching the final extreme, the microbial eukaryote, oxymonad *Monocercomonoides*, has no  
 331 mitochondrion whatsoever and lacks all typical nuclear-encoded mitochondrial proteins, showing that  
 332 while in 99% of organisms mitochondria play a vital role, this organelle is not indispensable  
 333 (Karnkowska *et al.* 2016).

334 In vertebrates but not all invertebrates, mtDNA is compact (16.5 kB in humans) and encodes 13  
 335 protein subunits of the transmembrane respiratory Complexes CI, CIII, CIV and ATP synthase (F-  
 336 ATPase), 22 tRNAs, and two RNAs. Additional gene content has been suggested to include microRNAs,  
 337 piRNA, smithRNAs, repeat associated RNA, and even additional proteins (Duarte *et al.* 2014; Lee *et al.*  
 338 2015; Cobb *et al.* 2016). The mitochondrial genome requires nuclear-encoded mitochondrially  
 339 targeted proteins, *e.g.*, TFAM, for its maintenance and expression (Rackham *et al.* 2012). Both genomes  
 340 encode peptides of the membrane spanning redox pumps (CI, CIII and CIV) and F-ATPase, leading to  
 341 strong constraints in the coevolution of both genomes (Blier *et al.* 2001).

342 Given the multiple roles of mitochondria, it is perhaps not surprising that mitochondrial  
 343 dysfunction is associated with a wide variety of genetic and degenerative diseases. Robust mitochondrial  
 344 function is supported by physical exercise and caloric balance, and is central for sustained metabolic  
 345 health throughout life. Therefore, a more consistent set of definitions for mitochondrial physiology will  
 346 increase our understanding of the etiology of disease and improve the diagnostic repertoire of  
 347 mitochondrial medicine with a focus on protective medicine, lifestyle and healthy aging.

348 Mitochondrion is singular and mitochondria is plural. Abbreviation: mt, as generally used in  
 349 mtDNA.

350

351

352

## 353 1. Introduction

354

355 Mitochondria are the powerhouses of the cell with numerous physiological, molecular, and  
 356 genetic functions (**Box 1**). Every study of mitochondrial health and disease faces Evolution, Age,  
 357 Gender and sex, Lifestyle, and Environment (MitoEAGLE) as essential background conditions intrinsic  
 358 to the individual person or cohort, species, tissue and to some extent even cell line. As a large and  
 359 coordinated group of laboratories and researchers, the mission of the global MitoEAGLE Network is to  
 360 generate the necessary scale, type, and quality of consistent data sets and conditions to address this  
 361 intrinsic complexity. Harmonization of experimental protocols and implementation of a quality control

362 and data management system are required to interrelate results gathered across a spectrum of studies  
363 and to generate a rigorously monitored database focused on mitochondrial respiratory function. In this  
364 way, researchers from a variety of disciplines can compare their findings using clearly defined and  
365 accepted international standards.

366 With an emphasis on quality of research, published data can be useful far beyond the specific  
367 question of a particular experiment. For example, collaborative data sets support the development of  
368 open-access databases such as those for National Institutes of Health sponsored research in genetics,  
369 proteomics, and metabolomics. Indeed, enabling meta-analysis is the most economic way of providing  
370 robust answers to biological questions (Cooper *et al.* 2009). However, the reproducibility of quantitative  
371 results and databases depend on accurate measurements under strictly-defined conditions. Likewise,  
372 meaningful interpretation and comparability of experimental outcomes requires standardisation of  
373 protocols between research groups at different institutes. In addition to quality control, a conceptual  
374 framework is also required to standardise and homogenise terminology and methodology. Vague or  
375 ambiguous jargon can lead to confusion and may convert valuable signals to wasteful noise. For this  
376 reason, measured values must be expressed in standard units for each parameter used to define  
377 mitochondrial respiratory function. A consensus on fundamental nomenclature and conceptual  
378 coherence, however, are missing in the expanding field of mitochondrial physiology. To fill this gap,  
379 the present communication provides an in-depth review on harmonization of nomenclature and  
380 definition of technical terms, which are essential to improve the awareness of the intricate meaning of  
381 current and past scientific vocabulary. This is important for documentation and integration into  
382 databases in general, and quantitative modelling in particular (Beard 2005).

383 In this review, we focus on coupling states and fluxes through metabolic pathways of aerobic  
384 energy transformation in mitochondrial preparations as a first step in the attempt to generate a  
385 conceptually-oriented nomenclature in bioenergetics and mitochondrial physiology. Respiratory control  
386 by fuel substrates and specific inhibitors of respiratory enzymes, coupling states of intact cells, and  
387 respiratory flux control ratios will be reviewed in subsequent communications, prepared in the frame of  
388 COST Action MitoEAGLE open to global bottom-up input.

389  
390

## 391 **2. Coupling states and rates in mitochondrial preparations**

392 *‘Every professional group develops its own technical jargon for talking about matters of critical*  
393 *concern ... People who know a word can share that idea with other members of their group, and*  
394 *a shared vocabulary is part of the glue that holds people together and allows them to create a*  
395 *shared culture’* (Miller 1991).

396

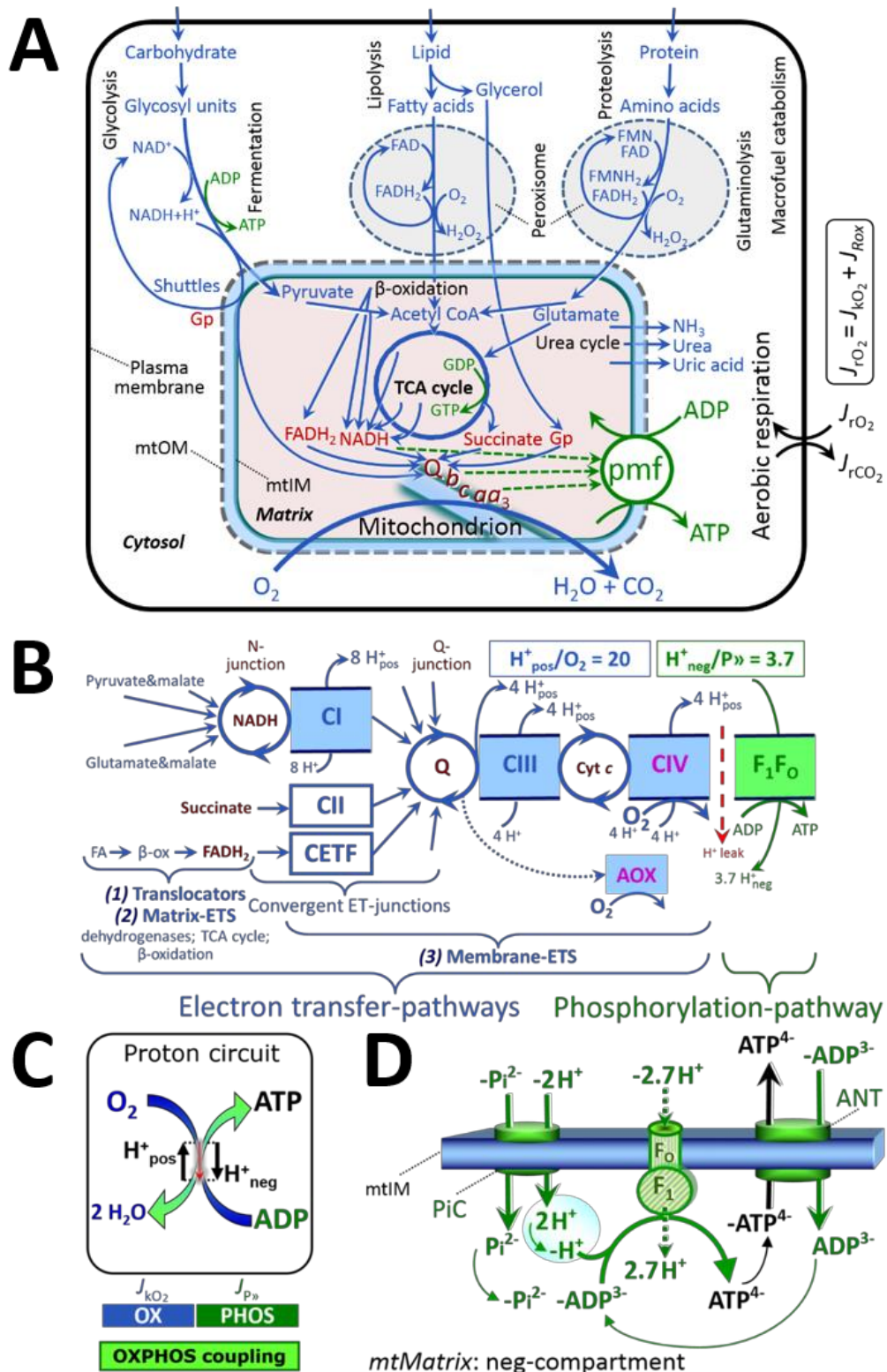
### 397 *2.1. Cellular and mitochondrial respiration*

398

399 **2.1.1. Aerobic and anaerobic catabolism and ATP turnover:** In respiration, electron transfer  
400 is coupled to the phosphorylation of ADP to ATP, with energy transformation mediated by the  
401 protonmotive force, pmf (**Figure 2**). Anabolic reactions are coupled to catabolism, both by ATP as the  
402 intermediary energy currency and by small organic precursor molecules as building blocks for  
403 biosynthesis. Glycolysis involves substrate-level phosphorylation of ADP to ATP in fermentation  
404 without utilization of O<sub>2</sub>, studied mainly in intact cells and organisms. Many cellular fuel substrates are  
405 catabolized to acetyl-CoA or to glutamate, and further electron transfer reduces nicotinamide adenine  
406 dinucleotide to NADH or flavin adenine dinucleotide to FADH<sub>2</sub>. Subsequent mitochondrial electron  
407 transfer to O<sub>2</sub> is coupled to proton translocation for the control of the protonmotive force and  
408 phosphorylation of ADP (**Figure 2B and 2C**). In contrast, extra-mitochondrial oxidation of fatty acids  
409 and amino acids proceeds partially in peroxisomes without coupling to ATP production: acyl-CoA  
410 oxidase catalyzes the oxidation of FADH<sub>2</sub> with electron transfer to O<sub>2</sub>; amino acid oxidases oxidize  
411 flavin mononucleotide FMNH<sub>2</sub> or FADH<sub>2</sub> (**Figure 2A**).

412





413  
414  
415  
416  
417  
418  
419  
420  
421  
422

423 **(B)** Respiration in mitochondrial preparations: The mitochondrial electron transfer system  
 424 (ETS) is (1) fuelled by diffusion and transport of substrates across the mtOM and mtIM,  
 425 and in addition consists of the (2) matrix-ETS, and (3) membrane-ETS. Electron transfer  
 426 converges at the N-junction, and from CI, CII and electron transferring flavoprotein  
 427 complex (CETF) at the Q-junction. Unlabeled arrows converging at the Q-junction indicate  
 428 additional ETS-sections with electron entry into Q through glycerophosphate  
 429 dehydrogenase, dihydro-orotate dehydrogenase, proline dehydrogenase, choline  
 430 dehydrogenase, and sulfide-ubiquinone oxidoreductase. The dotted arrow indicates the  
 431 branched pathway of oxygen consumption by alternative quinol oxidase (AOX). ET-  
 432 pathways are coupled to the phosphorylation-pathway. The  $H^+_{\text{pos}}/O_2$  ratio is the outward  
 433 proton flux from the matrix space to the positively (pos) charged vesicular compartment,  
 434 divided by catabolic  $O_2$  flux in the NADH-pathway. The  $H^+_{\text{neg}}/P_{\text{P}}$  ratio is the inward proton  
 435 flux from the inter-membrane space to the negatively (neg) charged matrix space, divided  
 436 by the flux of phosphorylation of ADP to ATP. These stoichiometries are not fixed because  
 437 of ion leaks and proton slip. Modified from Lemieux *et al.* (2017) and Rich (2013).  
 438 **(C)** OXPHOS coupling:  $O_2$  flux through the catabolic ET-pathway,  $J_{kO_2}$ , is coupled  
 439 by the  $H^+$  circuit to flux through the phosphorylation-pathway of ADP to ATP,  $J_{P_{\text{P}}}$ .  
 440 **(D)** Chemiosmotic phosphorylation-pathway catalyzed by the proton pump  $F_1F_0$ -ATPase  
 441 (F-ATPase, ATP synthase), adenine nucleotide translocase (ANT), and inorganic  
 442 phosphate carrier (PiC). The  $H^+_{\text{neg}}/P_{\text{P}}$  stoichiometry is the sum of the coupling  
 443 stoichiometry in the F-ATPase reaction ( $-2.7 H^+_{\text{pos}}$  from the positive intermembrane space,  
 444  $2.7 H^+_{\text{neg}}$  to the matrix, *i.e.*, the negative compartment) and the proton balance in the  
 445 translocation of  $ADP^{3-}$ ,  $ATP^{4-}$  and  $P_i^{2-}$ . Modified from Gnaiger (2014).  
 446

447 The plasma membrane separates the intracellular compartment including the cytosol, nucleus, and  
 448 organelles from the extracellular environment. The plasma membrane consists of a lipid bilayer with  
 449 embedded proteins and attached organic molecules that collectively control the selective permeability  
 450 of ions, organic molecules, and particles across the cell boundary. The intact plasma membrane prevents  
 451 the passage of many water-soluble mitochondrial substrates and inorganic ions—such as succinate,  
 452 adenosine diphosphate (ADP) and inorganic phosphate ( $P_i$ ) that must be precisely controlled at  
 453 kinetically-saturating concentrations for the analysis of mitochondrial respiratory capacities.  
 454 Respiratory capacities delineate, comparable to channel capacity in information theory (Schneider  
 455 2006), the upper boundary of the rate of  $O_2$  consumption measured in defined respiratory states. Despite  
 456 the activity of solute carriers, *e.g.*, SLC13A3 and SLC20A2, which transport specific metabolites across  
 457 the plasma membrane of various cell types, the intact plasma membrane limits the scope of  
 458 investigations into mitochondrial respiratory function in intact cells.

459 **2.1.2. Specification of biochemical dose:** Substrates, uncouplers, inhibitors, and other chemical  
 460 reagents are titrated to analyse cellular and mitochondrial function. Nominal concentrations of these  
 461 substances are usually reported as initial amount of substance concentration [ $\text{mol}\cdot\text{L}^{-1}$ ] in the incubation  
 462 medium. When aiming at the measurement of kinetically saturated processes—such as OXPHOS-  
 463 capacities—the concentrations for substrates can be chosen according to the apparent equilibrium  
 464 constant,  $K_m'$ . In the case of hyperbolic kinetics, only 80% of maximum respiratory capacity is obtained  
 465 at a substrate concentration of four times the  $K_m'$ , whereas substrate concentrations of 5, 9, 19 and 49  
 466 times the  $K_m'$  are theoretically required for reaching 83%, 90%, 95% or 98% of the maximal rate  
 467 (Gnaiger 2001). Other reagents are chosen to inhibit or alter a particular process. The amount of these  
 468 chemicals in an experimental incubation is selected to maximize effect, avoiding unacceptable off-target  
 469 consequences that would adversely affect the data being sought. Specifying the amount of substance in  
 470 an incubation as nominal concentration in the aqueous incubation medium can be ambiguous (Doskey  
 471 *et al.* 2015), particularly for cations ( $TPP^+$ ; fluorescent dyes such as safranin, TMRM; Chowdhury *et al.*  
 472 2015) and lipophilic substances (oligomycin, uncouplers, permeabilization agents; Doerrier *et al.* 2018),  
 473 which accumulate in the mitochondrial matrix or in biological membranes, respectively. Generally,  
 474 dose/exposure can be specified per unit of biological sample, *i.e.*, (nominal moles of  
 475 xenobiotic)/(number of cells) [ $\text{mol}\cdot\text{cell}^{-1}$ ] or, as appropriate, per mass of biological sample [ $\text{mol}\cdot\text{kg}^{-1}$ ].  
 476 This approach to specification of dose/exposure provides a scalable parameter that can be used to design  
 477 experiments, help interpret a wide variety of experimental results, and provide absolute information that  
 478 allows researchers worldwide to make the most use of published data (Doskey *et al.* 2015).

## 479 2.2. Mitochondrial preparations

480

481 Mitochondrial preparations are defined as either isolated mitochondria or tissue and cellular  
 482 preparations in which the barrier function of the plasma membrane is disrupted. Since this entails the  
 483 loss of cell viability, mitochondrial preparations are not studied *in vivo*. In contrast to isolated  
 484 mitochondria and tissue homogenate preparations, mitochondria in permeabilized tissues and cells are  
 485 *in situ* relative to the plasma membrane. When studying mitochondrial preparations, substrate-  
 486 uncoupler-inhibitor-titration (SUIT) protocols are used to establish respiratory coupling control states  
 487 (CCS) and pathway control states (PCS) that provide reference values for various output variables  
 488 (**Table 1**). Physiological conditions *in vivo* deviate from these experimentally obtained states; this is  
 489 because kinetically-saturating concentrations, *e.g.*, of ADP, oxygen (O<sub>2</sub>; dioxygen) or fuel substrates,  
 490 may not apply to physiological intracellular conditions. Further information is obtained in studies of  
 491 kinetic responses to variations in fuel substrate concentrations, [ADP], or [O<sub>2</sub>] in the range between  
 492 kinetically-saturating concentrations and anoxia (Gnaiger 2001).

493 The cholesterol content of the plasma membrane is high compared to mitochondrial membranes  
 494 (Korn 1969). Therefore, mild detergents—such as digitonin and saponin—can be applied to selectively  
 495 permeabilize the plasma membrane via interaction with cholesterol; this allows free exchange of organic  
 496 molecules and inorganic ions between the cytosol and the immediate cell environment, while  
 497 maintaining the integrity and localization of organelles, cytoskeleton, and the nucleus. Application of  
 498 permeabilization agents (mild detergents or toxins) leads to washout of cytosolic marker enzymes—  
 499 such as lactate dehydrogenase—and results in the complete loss of cell viability (tested by nuclear  
 500 staining using plasma membrane-impermeable dyes), while mitochondrial function remains intact  
 501 (tested by cytochrome *c* stimulation of respiration). Digitonin concentrations have to be optimized  
 502 according to cell type, particularly since mitochondria from cancer cells contain significantly higher  
 503 contents of cholesterol in both membranes (Baggetto and Testa-Perussini, 1990). For example, a dose  
 504 of digitonin of 8 fmol·cell<sup>-1</sup> (10 pg·cell<sup>-1</sup>; 10 μg·10<sup>-6</sup> cells) is optimal for permeabilization of endothelial  
 505 cells, and the concentration in the incubation medium has to be adjusted according to the cell density  
 506 (Doerrier *et al.* 2018). Respiration of isolated mitochondria remains unaltered after the addition of low  
 507 concentrations of digitonin or saponin. In addition to mechanical cell disruption during homogenization  
 508 of tissue, permeabilization agents may be applied to ensure permeabilization of all cells in tissue  
 509 homogenates.

510 Suspensions of cells permeabilized in the respiration chamber and crude tissue homogenates  
 511 contain all components of the cell at highly dilute concentrations. All mitochondria are retained in  
 512 chemically-permeabilized mitochondrial preparations and crude tissue homogenates. In the preparation  
 513 of isolated mitochondria, however, the mitochondria are separated from other cell fractions and purified  
 514 by differential centrifugation, entailing the loss of mitochondria at typical recoveries ranging from 30%  
 515 to 80% of total mitochondrial content (Lai *et al.* 2018). Using Percoll or sucrose density gradients to  
 516 maximize the purity of isolated mitochondria may compromise the mitochondrial yield or structural and  
 517 functional integrity. Therefore, mitochondrial isolation protocols need to be optimized according to each  
 518 study. The term, *mitochondrial preparation*, neither includes intact cells, nor submitochondrial particles  
 519 and further fractionation of mitochondrial components.

520

## 521 2.3. Electron transfer pathways

522

523 Mitochondrial electron transfer (ET) pathways are fuelled by diffusion and transport of substrates  
 524 across the mtOM and mtIM. In addition, the mitochondrial electron transfer system (ETS) consists of  
 525 the matrix-ETS and membrane-ETS (**Figure 2B**). Upstream sections of ET-pathways converge at the  
 526 NADH-junction (N-junction). NADH is mainly generated in the tricarboxylic acid (TCA) cycle and is  
 527 oxidized by Complex I (CI), with further electron entry into the coenzyme Q-junction (Q-junction).  
 528 Similarly, succinate is formed in the TCA cycle and oxidized by CII to fumarate. CII is part of both the  
 529 TCA cycle and the ETS, and reduces FAD to FADH<sub>2</sub> with further reduction of ubiquinone to ubiquinol  
 530 downstream of the TCA cycle in the Q-junction. Thus FADH<sub>2</sub> is not a substrate but is the product of  
 531 CII, in contrast to erroneous metabolic maps shown in many publications. β-oxidation of fatty acids  
 532 (FA) supplies reducing equivalents via (1) FADH<sub>2</sub> as the substrate of electron transferring flavoprotein  
 533 complex (ETF); (2) acetyl-CoA generated by chain shortening; and (3) NADH generated via 3-



534 hydroxyacyl-CoA dehydrogenases. The ATP yield depends on whether acetyl-CoA enters the TCA  
535 cycle, or is for example used in ketogenesis.

536 Selected mitochondrial catabolic pathways,  $k$ , of electron transfer from the oxidation of fuel  
537 substrates to the reduction of  $O_2$  are activated by addition of fuel substrates to the mitochondrial  
538 respiration medium after depletion of endogenous substrates (**Figure 2B**). Substrate combinations and  
539 specific inhibitors of ET-pathway enzymes are used to obtain defined pathway control states in  
540 mitochondrial preparations (Gnaiger 2014).

541

## 542 2.4. Respiratory coupling control

543

544 **2.4.1. Coupling:** In mitochondrial electron transfer, vectorial transmembrane proton flux is  
545 coupled through the redox proton pumps CI, CIII and CIV to the catabolic flux of scalar reactions,  
546 collectively measured as  $O_2$  flux,  $J_{kO_2}$  (**Figure 2**). Thus mitochondria are elementary components of  
547 energy transformation. Energy is a conserved quantity and cannot be lost or produced in any internal  
548 process (First Law of Thermodynamics). Open and closed systems can gain or lose energy only by  
549 external fluxes—by exchange with the environment. Therefore, energy can neither be produced by  
550 mitochondria, nor is there any internal process without energy conservation. Exergy or Gibbs energy  
551 (‘free energy’) is the part of energy that can potentially be transformed into work under conditions of  
552 constant temperature and pressure. *Coupling* is the interaction of an exergonic process (spontaneous,  
553 negative exergy change) with an endergonic process (positive exergy change) in energy transformations  
554 which conserve part of the exergy that would be irreversibly lost or dissipated in an uncoupled process.

555 Pathway control states (PCS) and coupling control states (CCS) are complementary, since  
556 mitochondrial preparations depend on (1) an exogenous supply of pathway-specific fuel substrates and  
557 oxygen, and (2) exogenous control of phosphorylation (**Figure 2**).

558 **2.4.2. Phosphorylation,  $P_{\gg}$ , and  $P_{\gg}/O_2$  ratio:** Phosphorylation in the context of OXPHOS is  
559 defined as phosphorylation of ADP by  $P_i$  to form ATP. On the other hand, the term phosphorylation is  
560 used generally in many contexts, *e.g.*, protein phosphorylation. This justifies consideration of a symbol  
561 more discriminating and specific than P as used in the P/O ratio (phosphate to atomic oxygen ratio),  
562 where P indicates phosphorylation of ADP to ATP or GDP to GTP (**Figure 2**). We propose the symbol  
563  $P_{\gg}$  for the endergonic (uphill) direction of phosphorylation  $ADP \rightarrow ATP$ , and likewise the symbol  $P_{\ll}$  for  
564 the corresponding exergonic (downhill) hydrolysis  $ATP \rightarrow ADP$ .  $P_{\gg}$  refers mainly to electrontransfer  
565 phosphorylation but may also involve substrate-level phosphorylation as part of the TCA cycle  
566 (succinyl-CoA ligase, phosphoglycerate kinase) and phosphorylation of ADP catalyzed by pyruvate  
567 kinase, and of GDP phosphorylated by phosphoenolpyruvate carboxykinase. Transphosphorylation is  
568 performed by adenylate kinase, creatine kinase (mtCK), hexokinase and nucleoside diphosphate kinase.  
569 In isolated mammalian mitochondria, ATP production catalyzed by adenylate kinase ( $2 ADP \leftrightarrow ATP +$   
570  $AMP$ ) proceeds without fuel substrates in the presence of ADP (Kömldi and Tretter 2017). Kinase  
571 cycles are involved in intracellular energy transfer and signal transduction for regulation of energy flux.

572 The  $P_{\gg}/O_2$  ratio ( $P_{\gg}/4 e^-$ ) is two times the ‘P/O’ ratio ( $P_{\gg}/2 e^-$ ).  $P_{\gg}/O_2$  is a generalized symbol, not  
573 specific for reporting  $P_i$  consumption ( $P_i/O_2$  flux ratio), ADP depletion ( $ADP/O_2$  flux ratio), or ATP  
574 production ( $ATP/O_2$  flux ratio). The mechanistic  $P_{\gg}/O_2$  ratio—or  $P_{\gg}/O_2$  stoichiometry—is calculated  
575 from the proton-to- $O_2$  and proton-to-phosphorylation coupling stoichiometries (**Figure 2B**):

$$577 \quad P_{\gg}/O_2 = \frac{H_{pos}^+/O_2}{H_{neg}^+/P_{\gg}} \quad (1)$$

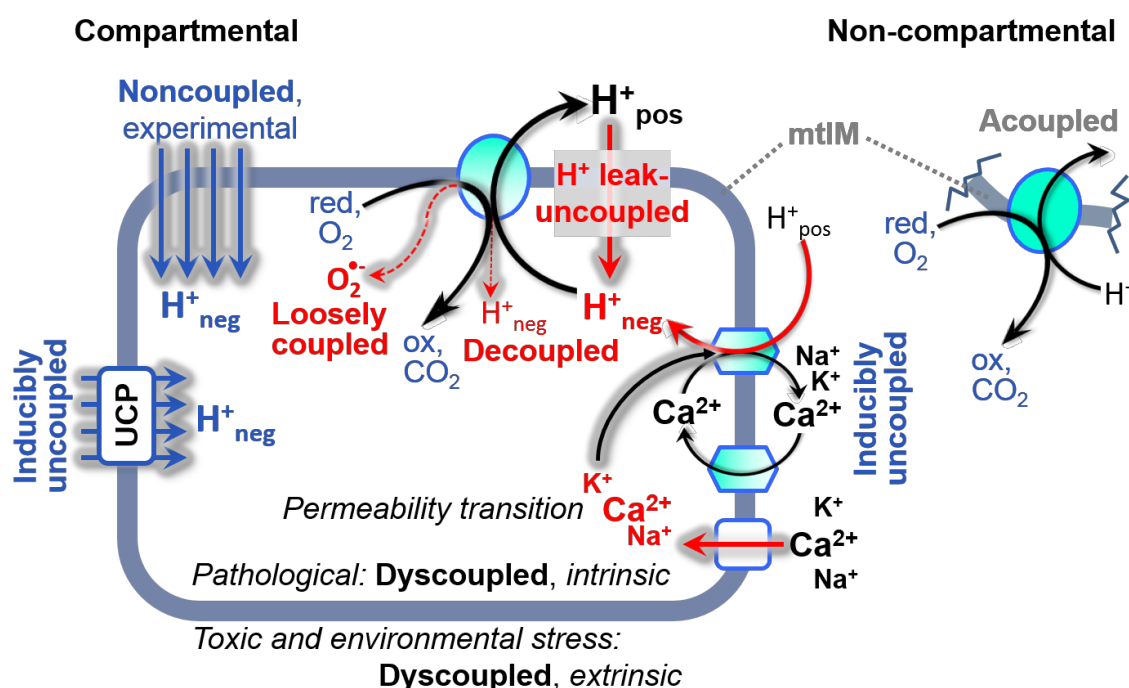
579 The  $H_{pos}^+/O_2$  coupling stoichiometry (referring to the full four electron reduction of  $O_2$ ) depends on the  
580 relative involvement of the three coupling sites (respiratory Complexes CI, CIII and CIV) in the  
581 catabolic ET-pathway from reduced fuel substrates (electron donors) to the reduction of  $O_2$  (electron  
582 acceptor). This varies with: (1) a bypass of CI by single or multiple electron input into the Q-junction;  
583 and (2) a bypass of CIV by involvement of alternative oxidases, AOX. AOX are expressed in all plants,  
584 some fungi, many protists, and several animal phyla, but are not expressed in vertebrate mitochondria  
585 (McDonald *et al.* 2009).

586 The  $H_{pos}^+/O_2$  coupling stoichiometry equals 12 in the ET-pathways involving CIII and CIV as  
587 proton pumps, increasing to 20 for the NADH-pathway through CI (**Figure 2B**), but a general consensus  
588 on  $H_{pos}^+/O_2$  stoichiometries remains to be reached (Hinkle 2005; Wikström and Hummer 2012; Sazanov  
589 2015). The  $H_{neg}^+/P_{\gg}$  coupling stoichiometry (3.7; **Figure 2B**) is the sum of 2.7  $H_{neg}^+$  required by the F-  
590 ATPase of vertebrate and most invertebrate species (Watt *et al.* 2010) and the proton balance in the



591 translocation of ADP, ATP and  $P_i$  (**Figure 2C**). Taken together, the mechanistic  $P_{\gg}/O_2$  ratio is calculated  
 592 at 5.4 and 3.3 for NADH- and succinate-linked respiration, respectively (Eq. 1). The corresponding  
 593 classical  $P_{\gg}/O$  ratios (referring to the 2 electron reduction of  $0.5 O_2$ ) are 2.7 and 1.6 (Watt *et al.* 2010),  
 594 in agreement with the measured  $P_{\gg}/O$  ratio for succinate of  $1.58 \pm 0.02$  (Gnaiger *et al.* 2000).

595 **2.4.3. Uncoupling:** The effective  $P_{\gg}/O_2$  flux ratio ( $Y_{P_{\gg}/O_2} = J_{P_{\gg}}/J_{kO_2}$ ) is diminished relative to the  
 596 mechanistic  $P_{\gg}/O_2$  ratio by intrinsic and extrinsic uncoupling or dyscoupling (**Figure 3**). Such  
 597 generalized uncoupling is different from switching to mitochondrial pathways that involve fewer than  
 598 three proton pumps ('coupling sites': Complexes CI, CIII and CIV), bypassing CI through multiple  
 599 electron entries into the Q-junction, or CIII and CIV through AOX (**Figure 2B**). Reprogramming of  
 600 mitochondrial pathways leading to different types of substrates being oxidized may be considered as a  
 601 switch of gears (changing the stoichiometry by altering the substrate that is oxidized) rather than  
 602 uncoupling (loosening the tightness of coupling relative to a fixed stoichiometry). In addition,  $Y_{P_{\gg}/O_2}$   
 603 depends on several experimental conditions of flux control, increasing as a hyperbolic function of [ADP]  
 604 to a maximum value (Gnaiger 2001).  
 605



606  
 607  
 608  
 609  
 610  
 611  
 612  
 613  
 614  
 615  
 616  
 617

### Figure 3. Mechanisms of respiratory uncoupling

An intact mitochondrial inner membrane, mtIM, is required for vectorial, compartmental coupling. 'Acoupled' respiration is the consequence of structural disruption with catalytic activity of non-compartmental mitochondrial fragments. Inducible uncoupling, *e.g.*, by activation of UCP1, increases LEAK-respiration; experimentally noncoupled respiration provides an estimate of ET-capacity obtained by titration of protonophores stimulating respiration to maximum  $O_2$  flux.  $H^+$  leak-uncoupled, decoupled, and loosely coupled respiration are components of intrinsic uncoupling (**Table 2**). Pathological dysfunction may affect all types of uncoupling, including permeability transition, causing intrinsically dyscoupled respiration. Similarly, toxicological and environmental stress factors can cause extrinsically dyscoupled respiration. Reduced fuel substrates, red; oxidized products, ox.

618 Uncoupling of mitochondrial respiration is a general term comprising diverse mechanisms:

- 619 1. Proton leak across the mtIM from the positive to the negative compartment ( $H^+$  leak-uncoupled;  
 620 **Figure 3**).
- 621 2. Cycling of other cations, strongly stimulated by permeability transition; comparable to the use of  
 622 protonophores, cation cycling is experimentally induced by valinomycin in the presence of  $K^+$ ;
- 623 3. Decoupling by proton slip in the redox proton pumps when protons are effectively not pumped  
 624 (CI, CIII and CIV) or are not driving phosphorylation (F-ATPase);
- 625 4. Loss of vesicular (compartmental) integrity when electron transfer is acoupled;

626 5. Electron leak in the loosely coupled univalent reduction of O<sub>2</sub> to superoxide (O<sub>2</sub><sup>•-</sup>; superoxide  
627 anion radical).  
628 Differences of terms—uncoupled *vs.* noncoupled—are easily overlooked, although they relate to  
629 different meanings of uncoupling (**Figure 3** and **Table 2**).

630

631 *2.5. Coupling states and respiratory rates*

632

633 To extend the classical nomenclature on mitochondrial coupling states (Section 2.6) by a concept-  
634 driven terminology that explicitly incorporates information on the meaning of respiratory states, the  
635 terminology must be general and not restricted to any particular experimental protocol or mitochondrial  
636 preparation (Gnaiger 2009). Concept-driven nomenclature aims at mapping the meaning and concept  
637 behind the words and acronyms onto the forms of words and acronyms (Miller 1991). The focus of  
638 concept-driven nomenclature is primarily the conceptual *why*, along with clarification of the  
639 experimental *how*.

640

641 **Table 1. Coupling states and residual oxygen consumption in mitochondrial**  
642 **preparations in relation to respiration- and phosphorylation-flux,  $J_{kO_2}$  and  $J_{P_{\gg}}$ , and**  
643 **protonmotive force, pmf.** Coupling states are established at kinetically-saturating  
644 concentrations of fuel substrates and O<sub>2</sub>.

State	$J_{kO_2}$	$J_{P_{\gg}}$	pmf	Inducing factors	Limiting factors
LEAK	<i>L</i> ; low, cation leak-dependent respiration	0	max.	back-flux of cations including proton leak, proton slip	$J_{P_{\gg}} = 0$ : (1) without ADP, $L_N$ ; (2) max. ATP/ADP ratio, $L_T$ ; or (3) inhibition of the phosphorylation-pathway, $L_{Omy}$
OXPHOS	<i>P</i> ; high, ADP-stimulated respiration, OXPHOS-capacity	max.	high	kinetically-saturating [ADP] and [P <sub>i</sub> ]	$J_{P_{\gg}}$ by phosphorylation-pathway capacity; or $J_{kO_2}$ by ET-capacity
ET	<i>E</i> ; max., noncoupled respiration, ET-capacity	0	low	optimal external uncoupler concentration for max. $J_{O_2,E}$	$J_{kO_2}$ by ET-capacity
ROX	<i>Rox</i> ; min., residual O <sub>2</sub> consumption	0	0	$J_{O_2,Rox}$ in non-ET-pathway oxidation reactions	inhibition of all ET-pathways; or absence of fuel substrates

645

646 To provide a diagnostic reference for respiratory capacities of core energy metabolism, the  
647 capacity of oxidative phosphorylation, OXPHOS, is measured at kinetically-saturating concentrations  
648 of ADP and P<sub>i</sub>. The oxidative ET-capacity reveals the limitation of OXPHOS-capacity mediated by the  
649 phosphorylation-pathway. The ET- and phosphorylation-pathways comprise coupled segments of the  
650 OXPHOS-system. By application of external uncouplers, ET-capacity is measured as noncoupled  
651 respiration. The contribution of intrinsically uncoupled O<sub>2</sub> consumption is studied by preventing the  
652 stimulation of phosphorylation either in the absence of ADP or by inhibition of the phosphorylation-  
653 pathway. The corresponding states are collectively classified as LEAK-states when O<sub>2</sub> consumption  
654 compensates mainly for ion leaks, including the proton leak. Defined coupling states are induced by: (1)  
655 adding cation chelators such as EGTA, binding free Ca<sup>2+</sup> and thus limiting cation cycling; (2) adding  
656 ADP and P<sub>i</sub>; (3) inhibiting the phosphorylation-pathway; and (4) uncoupler titrations, while maintaining  
657 a defined ET-pathway state with constant fuel substrates and inhibitors of specific branches of the ET-  
658 pathway.

659

660 The three coupling states, ET, LEAK and OXPHOS, are shown schematically with the  
661 corresponding respiratory rates, abbreviated as *E*, *L* and *P*, respectively (**Figure 4**). We distinguish  
662 metabolic *pathways* from metabolic *states* and the corresponding metabolic *rates*; for example: ET-

662 pathways, ET-states, and ET-capacities,  $E$ , respectively (Table 1). The protonmotive force is *high* in  
 663 the OXPHOS-state when it drives phosphorylation, *maximum* in the LEAK-state of coupled  
 664 mitochondria, driven by LEAK-respiration at a minimum back-flux of cations to the matrix side, and  
 665 *very low* in the ET-state when uncouplers short-circuit the proton cycle (Table 1).

666

667 **Figure 4. Four-compartment**  
 668 **model of oxidative**  
 669 **phosphorylation**

670 Respiratory states (ET, OXPHOS,  
 671 LEAK; Table 1) and corresponding  
 672 rates ( $E$ ,  $P$ ,  $L$ ) are connected by the  
 673 protonmotive force, pmf. (1) ET-  
 674 capacity,  $E$ , is partitioned into (2)  
 675 dissipative LEAK-respiration,  $L$ ,  
 676 when the Gibbs energy change of  
 677 catabolic  $O_2$  flux is irreversibly lost,  
 678 (3) net OXPHOS-capacity,  $P-L$ , with  
 679 partial conservation of the capacity to perform work, and (4) the excess capacity,  $E-P$ . Modified from  
 680 Gnaiger (2014).

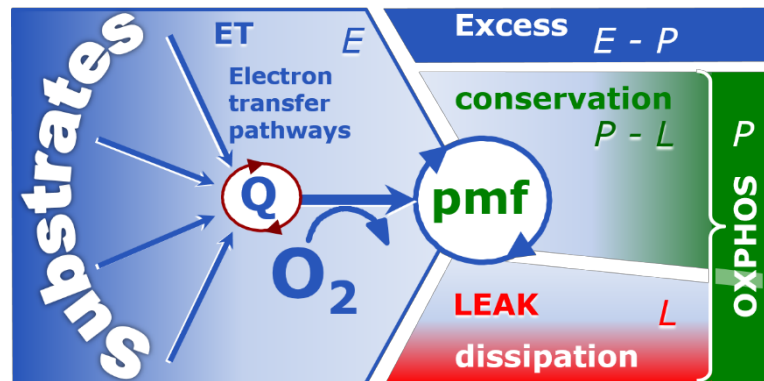
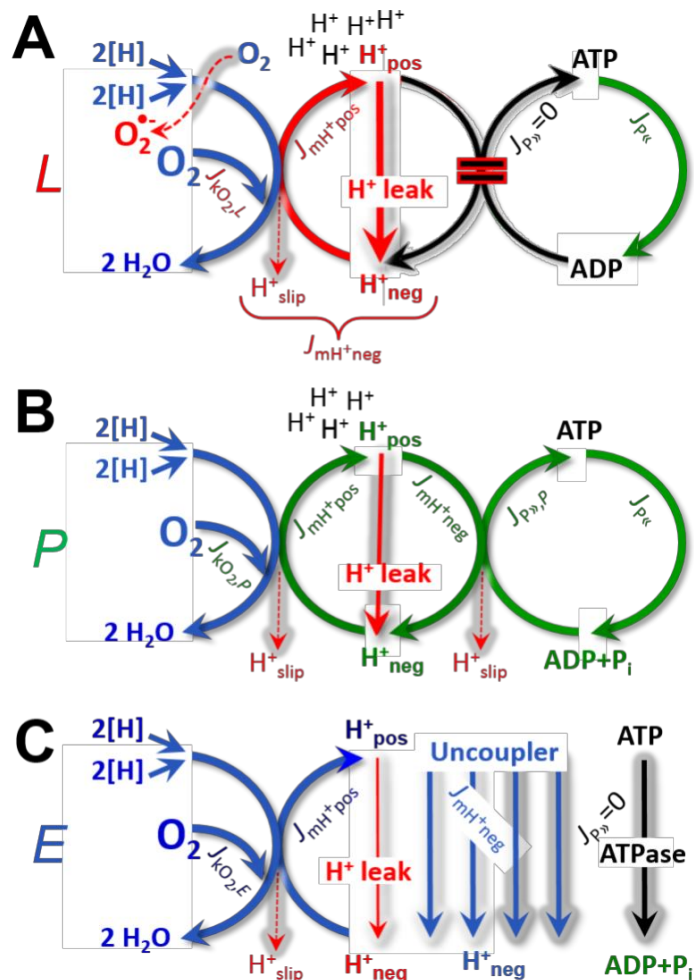


**Figure 5. Respiratory coupling states**

**(A) LEAK-state and rate,  $L$ :** Oxidation only, since phosphorylation is arrested,  $J_{P\gg} = 0$ , and catabolic  $O_2$  flux,  $J_{kO_2,L}$ , is controlled mainly by the proton leak and slip,  $J_{mH^+neg}$ , at maximum protonmotive force (Figure 4). Extramitochondrial ATPases,  $J_{P\ll}$ ; then phosphorylation must be blocked.

**(B) OXPHOS-state and rate,  $P$ :** Oxidation coupled to phosphorylation,  $J_{P\gg}$ , which is stimulated by kinetically-saturating [ADP] and  $[P_i]$ , supported by a high protonmotive force.  $O_2$  flux,  $J_{kO_2,P}$ , is well-coupled at a  $P\gg/O_2$  ratio of  $J_{P\gg,P}/J_{O_2,P}$ . Extramitochondrial ATPases may recycle ATP,  $J_{P\ll}$ .

**(C) ET-state and rate,  $E$ :** Oxidation only, since phosphorylation is zero,  $J_{P\gg} = 0$ , at optimum exogenous uncoupler concentration when noncoupled respiration,  $J_{kO_2,E}$ , is maximum. The F-ATPase may hydrolyze extramitochondrial ATP.



681

682

683 **2.5.1. LEAK-state (Figure 5A):** The LEAK-state is defined as a state of mitochondrial  
 684 respiration when  $O_2$  flux mainly compensates for ion leaks in the absence of ATP synthesis, at  
 685 kinetically-saturating concentrations of  $O_2$ , respiratory fuel substrates and  $P_i$ . LEAK-respiration is  
 measured to obtain an estimate of intrinsic uncoupling without addition of an experimental uncoupler:

686 (1) in the absence of adenylates, *i.e.*, AMP, ADP and ATP; (2) after depletion of ADP at a maximum  
 687 ATP/ADP ratio; or (3) after inhibition of the phosphorylation-pathway by inhibitors of F-ATPase—such  
 688 as oligomycin, or of adenine nucleotide translocase—such as carboxyatractyloside. Adjustment of the  
 689 nominal concentration of these inhibitors to the density of biological sample applied can minimize or  
 690 avoid inhibitory side-effects exerted on ET-capacity or even some dyscoupling.  
 691  
 692

**Table 2. Terms on respiratory coupling and uncoupling.**

Term	$J_{kO_2}$	$P \gg O_2$	Notes	
acoupled		0	electron transfer in mitochondrial fragments without vectorial proton translocation ( <b>Figure 3</b> )	
intrinsic, no protonophore added	uncoupled	$L$	0	non-phosphorylating <b>LEAK-respiration</b> ( <b>Figure 5A</b> )
			0	component of $L$ , $H^+$ diffusion across the mtIM ( <b>Figure 3</b> )
			0	component of $L$ , proton slip ( <b>Figure 3</b> )
			0	component of $L$ , lower coupling due to superoxide formation and bypass of proton pumps by electron leak ( <b>Figure 3</b> )
			0	pathologically, toxicologically, environmentally increased uncoupling, mitochondrial dysfunction
			0	by UCP1 or cation ( <i>e.g.</i> , $Ca^{2+}$ ) cycling ( <b>Figure 3</b> )
noncoupled	$E$	0	ET-capacity, non-phosphorylating respiration stimulated to maximum flux at optimum exogenous protonophore concentration ( <b>Figure 5C</b> )	
well-coupled	$P$	high	<b>OXPPOS-capacity</b> , phosphorylating respiration with an intrinsic LEAK component ( <b>Figure 5B</b> )	
fully coupled	$P - L$	max.	<b>OXPPOS-capacity</b> corrected for LEAK-respiration ( <b>Figure 4</b> )	

693

694

695

696

697

698

699

700

701

702

703

704

705

706

707

708

709

710

711

712

713

714

- **Proton leak and uncoupled respiration:** The intrinsic proton leak is the *uncoupled* leak current of protons in which protons diffuse across the mtIM in the dissipative direction of the downhill protonmotive force without coupling to phosphorylation (**Figure 5A**). The proton leak flux depends non-linearly on the protonmotive force (Garlid *et al.* 1989; Divakaruni and Brand 2011), which is a temperature-dependent property of the mtIM and may be enhanced due to possible contamination by free fatty acids. Inducible uncoupling mediated by uncoupling protein 1 (UCP1) is physiologically controlled, *e.g.*, in brown adipose tissue. UCP1 is a member of the mitochondrial carrier family that is involved in the translocation of protons across the mtIM (Klingenberg 2017). Consequently, this short-circuit lowers the protonmotive force and stimulates electron transfer, respiration, and heat dissipation in the absence of phosphorylation of ADP.
- **Cation cycling:** There can be other cation contributors to leak current including calcium and probably magnesium. Calcium influx is balanced by mitochondrial  $Na^+/Ca^{2+}$  or  $H^+/Ca^{2+}$  exchange, which is balanced by  $Na^+/H^+$  or  $K^+/H^+$  exchanges. This is another effective uncoupling mechanism different from proton leak (**Table 2**).
- **Proton slip and decoupled respiration:** Proton slip is the *decoupled* process in which protons are only partially translocated by a redox proton pump of the ET-pathways and slip back to the original vesicular compartment. The proton leak is the dominant contributor to the overall leak current in mammalian mitochondria incubated under physiological conditions at 37 °C, whereas proton slip increases at lower experimental temperature (Canton *et al.* 1995). Proton slip can also happen in association with the F-ATPase, in which the proton slips downhill across the pump to



715 the matrix without contributing to ATP synthesis. In each case, proton slip is a property of the  
716 proton pump and increases with the pump turnover rate.

- 717 • **Electron leak and loosely coupled respiration:** Superoxide production by the ETS leads to a  
718 bypass of redox proton pumps and correspondingly lower  $P_{\gg}/O_2$  ratio. This depends on the actual  
719 site of electron leak and the scavenging of hydrogen peroxide by cytochrome *c*, whereby electrons  
720 may re-enter the ETS with proton translocation by CIV.
- 721 • **Loss of compartmental integrity and acoupled respiration:** Electron transfer and catabolic  $O_2$   
722 flux proceed without compartmental proton translocation in disrupted mitochondrial fragments.  
723 Such fragments are an artefact of mitochondrial isolation, and may not fully fuse to re-establish  
724 structurally intact mitochondria. Loss of mtIM integrity, therefore, is the cause of acoupled  
725 respiration, which is a nonvectorial dissipative process without control by the protonmotive force.
- 726 • **Dyscoupled respiration:** Mitochondrial injuries may lead to *dyscoupling* as a pathological or  
727 toxicological cause of *uncoupled* respiration. Dyscoupling may involve any type of uncoupling  
728 mechanism, *e.g.*, opening the permeability transition pore. Dyscoupled respiration is  
729 distinguished from the experimentally induced *noncoupled* respiration in the ET-state (**Table 2**).

730

731 **2.5.2. OXPHOS-state (Figure 5B):** The OXPHOS-state is defined as the respiratory state with  
732 kinetically-saturating concentrations of  $O_2$ , respiratory and phosphorylation substrates, and absence of  
733 exogenous uncoupler, which provides an estimate of the maximal respiratory capacity in the OXPHOS-  
734 state for any given ET-pathway state. Respiratory capacities at kinetically-saturating substrate  
735 concentrations provide reference values or upper limits of performance, aiming at the generation of data  
736 sets for comparative purposes. Physiological activities and effects of substrate kinetics can be evaluated  
737 relative to the OXPHOS-capacity.

738 As discussed previously, 0.2 mM ADP does not fully saturate flux in isolated mitochondria  
739 (Gnaiger 2001; Puchowicz *et al.* 2004); greater [ADP] is required, particularly in permeabilized muscle  
740 fibres and cardiomyocytes, to overcome limitations by intracellular diffusion and by the reduced  
741 conductance of the mtOM (Jepihhina *et al.* 2011; Illaste *et al.* 2012; Simson *et al.* 2016), either through  
742 interaction with tubulin (Rostovtseva *et al.* 2008) or other intracellular structures (Birkedal *et al.* 2014).  
743 In addition, saturating ADP concentrations need to be evaluated under different experimental conditions  
744 such as temperature (Lemieux *et al.* 2017) and with different animal models (Blier and Guderley, 1993).  
745 In permeabilized muscle fibre bundles of high respiratory capacity, the apparent  $K_m$  for ADP increases  
746 up to 0.5 mM (Saks *et al.* 1998), consistent with experimental evidence that >90% saturation is reached  
747 only at >5 mM ADP (Pesta and Gnaiger 2012). Similar ADP concentrations are also required for  
748 accurate determination of OXPHOS-capacity in human clinical cancer samples and permeabilized cells  
749 (Klepinin *et al.* 2016; Koit *et al.* 2017). 2.5 to 5 mM ADP is sufficient to obtain the actual OXPHOS-  
750 capacity in many types of permeabilized tissue and cell preparations, but experimental validation is  
751 required in each specific case.

752 **2.5.3. Electron transfer-state (Figure 5C):**  $O_2$  flux determined in the ET-state yields an estimate  
753 of ET-capacity. The ET-state is defined as the *noncoupled* state with kinetically-saturating  
754 concentrations of  $O_2$ , respiratory substrate and optimum exogenous uncoupler concentration for  
755 maximum  $O_2$  flux. Uncouplers are weak lipid-soluble acids which function as protonophores. These  
756 disrupt the barrier function of the mtIM and thus short circuit the protonmotive system, functioning like  
757 a clutch in a mechanical system. As a consequence of the nearly collapsed protonmotive force, the  
758 driving force is insufficient for phosphorylation, and  $J_{P_{\gg}} = 0$ . The most frequently used uncouplers are  
759 carbonyl cyanide *m*-chloro phenyl hydrazone (CCCP), carbonyl cyanide *p*-  
760 trifluoromethoxyphenylhydrazone (FCCP), or dinitrophenol (DNP). Stepwise titration of uncouplers  
761 stimulates respiration up to or above the level of  $O_2$  consumption rates in the OXPHOS-state; respiration  
762 is inhibited, however, above optimum uncoupler concentrations (Mitchell 2011). Data obtained with a  
763 single dose of uncoupler must be evaluated with caution, particularly when a fixed uncoupler  
764 concentration is used in studies exploring a treatment or disease that may alter the mitochondrial content  
765 or mitochondrial sensitivity to inhibition by uncouplers. The effect on ET-capacity of the reversed  
766 function of F-ATPase ( $J_{P_{\ll}}$ ; **Figure 5C**) can be evaluated in the presence and absence of  
767 extramitochondrial ATP.

768 **2.5.4. ROX state and *Rox*:** Besides the three fundamental coupling states of mitochondrial  
769 preparations, the state of residual  $O_2$  consumption, ROX, which although not a coupling state, is relevant  
770 to assess respiratory function (**Figure 1**). The rate of residual oxygen consumption, *Rox*, is defined as

771 O<sub>2</sub> consumption due to oxidative reactions measured after inhibition of ET with rotenone, malonic acid  
 772 and antimycin A. Cyanide and azide inhibit not only CIV but catalase and several peroxidases involved  
 773 in *Rox*. High concentrations of antimycin A, but not rotenone or cyanide, inhibit peroxisomal acyl-CoA  
 774 oxidase and D-amino acid oxidase (Vamecq *et al.* 1987). *Rox* represents a baseline used to correct  
 775 respiration measured in defined coupling control states. *Rox*-corrected *L*, *P* and *E* not only lower the  
 776 values of total fluxes, but also change the flux control ratios *L/P* and *L/E*. *Rox* is not necessarily  
 777 equivalent to non-mitochondrial reduction of O<sub>2</sub>, considering O<sub>2</sub>-consuming reactions in mitochondria  
 778 that are not related to ET—such as O<sub>2</sub> consumption in reactions catalyzed by monoamine oxidases (type  
 779 A and B), monooxygenases (cytochrome P450 monooxygenases), dioxygenase (sulfur dioxygenase and  
 780 trimethyllysine dioxygenase), and several hydroxylases. Even isolated mitochondrial fractions,  
 781 especially those obtained from liver, may be contaminated by peroxisomes, as shown by transmission  
 782 electron microscopy. This fact makes the exact determination of mitochondrial O<sub>2</sub> consumption and  
 783 mitochondria-associated generation of reactive oxygen species complicated (Schönfeld *et al.* 2009;  
 784 Speijer 2016; **Figure 2**). The dependence of ROX-linked O<sub>2</sub> consumption needs to be studied in detail  
 785 together with non-ET enzyme activities, availability of specific substrates, O<sub>2</sub> concentration, and  
 786 electron leakage leading to the formation of reactive oxygen species.

787 **2.5.5. Quantitative relations:** *E* may exceed or be equal to *P*.  $E > P$  is observed in many types  
 788 of mitochondria, varying between species, tissues and cell types (Gnaiger 2009). *E-P* is the excess ET-  
 789 capacity pushing the phosphorylation-flux (**Figure 2C**) to the limit of its capacity for utilizing the  
 790 protonmotive force. In addition, the magnitude of *E-P* depends on the tightness of respiratory coupling  
 791 or degree of uncoupling, since an increase of *L* causes *P* to increase towards the limit of *E*. The excess  
 792 *E-P* capacity, *E-P*, therefore, provides a sensitive diagnostic indicator of specific injuries of the  
 793 phosphorylation-pathway, under conditions when *E* remains constant but *P* declines relative to controls  
 794 (**Figure 4**). Substrate cocktails supporting simultaneous convergent electron transfer to the Q-junction  
 795 for reconstitution of TCA cycle function establish pathway control states with high ET-capacity, and  
 796 consequently increase the sensitivity of the *E-P* assay.

797 *E* cannot theoretically be lower than *P*.  $E < P$  must be discounted as an artefact, which may be  
 798 caused experimentally by: (1) loss of oxidative capacity during the time course of the respirometric  
 799 assay, since *E* is measured subsequently to *P*; (2) using insufficient uncoupler concentrations; (3) using  
 800 high uncoupler concentrations which inhibit ET (Gnaiger 2008); (4) high oligomycin concentrations  
 801 applied for measurement of *L* before titrations of uncoupler, when oligomycin exerts an inhibitory effect  
 802 on *E*. On the other hand, the excess ET-capacity is overestimated if non-saturating [ADP] or [P<sub>i</sub>] are  
 803 used. See State 3 in the next section.

804 The net OXPHOS-capacity is calculated by subtracting *L* from *P* (**Figure 4**). The net P<sub>»</sub>/O<sub>2</sub> equals  
 805  $P_{»}/(P-L)$ , wherein the dissipative LEAK component in the OXPHOS-state may be overestimated. This  
 806 can be avoided by measuring LEAK-respiration in a state when the protonmotive force is adjusted to its  
 807 slightly lower value in the OXPHOS-state by titration of an ET inhibitor (Divakaruni and Brand 2011).  
 808 Any turnover-dependent components of proton leak and slip, however, are underestimated under these  
 809 conditions (Garlid *et al.* 1993). In general, it is inappropriate to use the term *ATP production* or *ATP*  
 810 *turnover* for the difference of O<sub>2</sub> flux measured in the OXPHOS and LEAK states. *P-L* is the upper limit  
 811 of OXPHOS-capacity that is freely available for ATP production (corrected for LEAK-respiration) and  
 812 is fully coupled to phosphorylation with a maximum mechanistic stoichiometry (**Figure 4**).

813 LEAK-respiration and OXPHOS-capacity depend on (1) the tightness of coupling under the  
 814 influence of the respiratory uncoupling mechanisms (**Figure 3**), and (2) the coupling stoichiometry,  
 815 which varies as a function of the substrate type undergoing oxidation in ET-pathways with either two  
 816 or three coupling sites (**Figure 2B**). When cocktails with NADH-linked substrates and succinate are  
 817 used, the relative contribution of ET-pathways with three or two coupling sites cannot be controlled  
 818 experimentally, is difficult to determine, and may shift in transitions between LEAK-, OXPHOS- and  
 819 ET-states (Gnaiger 2014). Under these experimental conditions, we cannot separate the tightness of  
 820 coupling *versus* coupling stoichiometry as the mechanisms of respiratory control in the shift of *L/P*  
 821 ratios. The tightness of coupling and fully coupled O<sub>2</sub> flux, *P-L* (**Table 2**), therefore, are obtained from  
 822 measurements of coupling control of LEAK-respiration, OXPHOS- and ET-capacities in well-defined  
 823 pathway states, using either pyruvate and malate as substrates or the classical succinate and rotenone  
 824 substrate-inhibitor combination (**Figure 2B**).

825 **2.5.6. The steady-state:** Mitochondria represent a thermodynamically open system in non-  
 826 equilibrium states of biochemical energy transformation. State variables (protonmotive force; redox

827 states) and metabolic *rates* (fluxes) are measured in defined mitochondrial respiratory *states*. Steady-  
 828 states can be obtained only in open systems, in which changes by internal transformations, *e.g.*, O<sub>2</sub>  
 829 consumption, are instantaneously compensated for by external fluxes, *e.g.*, O<sub>2</sub> supply, preventing a  
 830 change of O<sub>2</sub> concentration in the system (Gnaiger 1993b). Mitochondrial respiratory states monitored  
 831 in closed systems satisfy the criteria of pseudo-steady states for limited periods of time, when changes  
 832 in the system (concentrations of O<sub>2</sub>, fuel substrates, ADP, P<sub>i</sub>, H<sup>+</sup>) do not exert significant effects on  
 833 metabolic fluxes (respiration, phosphorylation). Such pseudo-steady states require respiratory media  
 834 with sufficient buffering capacity and substrates maintained at kinetically-saturating concentrations, and  
 835 thus depend on the kinetics of the processes under investigation.

836

### 837 2.6. Classical terminology for isolated mitochondria

838 *'When a code is familiar enough, it ceases appearing like a code; one forgets that there is a*  
 839 *decoding mechanism. The message is identical with its meaning'* (Hofstadter 1979).

840

841 Chance and Williams (1955; 1956) introduced five classical states of mitochondrial respiration  
 842 and cytochrome redox states. **Table 3** shows a protocol with isolated mitochondria in a closed  
 843 respirometric chamber, defining a sequence of respiratory states. States and rates are not specifically  
 844 distinguished in this nomenclature.

845

846

**Table 3. Metabolic states of mitochondria (Chance and Williams, 1956; Table V).**

847

848

State	[O <sub>2</sub> ]	ADP level	Substrate level	Respiration rate	Rate-limiting substance
1	>0	low	low	slow	ADP
2	>0	high	~0	slow	substrate
3	>0	high	high	fast	respiratory chain
4	>0	low	high	slow	ADP
5	0	high	high	0	oxygen

849

850 **2.6.1. State 1** is obtained after addition of isolated mitochondria to air-saturated  
 851 isoosmotic/isotonic respiration medium containing P<sub>i</sub>, but no fuel substrates and no adenylates.

852 **2.6.2. State 2** is induced by addition of a 'high' concentration of ADP (typically 100 to 300 μM),  
 853 which stimulates respiration transiently on the basis of endogenous fuel substrates and phosphorylates  
 854 only a small portion of the added ADP. State 2 is then obtained at a low respiratory activity limited by  
 855 exhausted endogenous fuel substrate availability (**Table 3**). If addition of specific inhibitors of  
 856 respiratory complexes such as rotenone does not cause a further decline of O<sub>2</sub> flux, State 2 is equivalent  
 857 to the ROX state (See below.). If inhibition is observed, undefined endogenous fuel substrates are a  
 858 confounding factor of pathway control, contributing to the effect of subsequently externally added  
 859 substrates and inhibitors. In contrast to the original protocol, an alternative sequence of titration steps is  
 860 frequently applied, in which the alternative 'State 2' has an entirely different meaning when this second  
 861 state is induced by addition of fuel substrate without ADP or ATP (LEAK-state; in contrast to State 2  
 862 defined in **Table 1** as a ROX state). Some researchers have called this condition as 'pseudostate 4'  
 863 because it has no significant concentrations of adenine nucleotides and hence it is not a near-  
 864 physiological condition, although it should be used for calculating the net OXPHOS-capacity, *P-L*.

865 **2.6.3. State 3** is the state stimulated by addition of fuel substrates while the ADP concentration  
 866 is still high (**Table 3**) and supports coupled energy transformation through oxidative phosphorylation.  
 867 'High ADP' is a concentration of ADP specifically selected to allow the measurement of State 3 to State  
 868 4 transitions of isolated mitochondria in a closed respirometric chamber. Repeated ADP titration re-  
 869 establishes State 3 at 'high ADP'. Starting at O<sub>2</sub> concentrations near air-saturation (193 or 238 μM O<sub>2</sub>  
 870 at 37 °C or 25 °C and sea level at 1 atm or 101.32 kPa, and an oxygen solubility of respiration medium  
 871 at 0.92 times that of pure water; Forstner and Gnaiger 1983), the total ADP concentration added must  
 872 be low enough (typically 100 to 300 μM) to allow phosphorylation to ATP at a coupled O<sub>2</sub> flux that  
 873 does not lead to O<sub>2</sub> depletion during the transition to State 4. In contrast, kinetically-saturating ADP

874 concentrations usually are 10-fold higher than 'high ADP', *e.g.*, 2.5 mM in isolated mitochondria. The  
 875 abbreviation State 3u is occasionally used in bioenergetics, to indicate the state of respiration after  
 876 titration of an uncoupler, without sufficient emphasis on the fundamental difference between OXPHOS-  
 877 capacity (*well-coupled* with an endogenous uncoupled component) and ET-capacity (*noncoupled*).

878 **2.6.4. State 4** is a LEAK-state that is obtained only if the mitochondrial preparation is intact and  
 879 well-coupled. Depletion of ADP by phosphorylation to ATP causes a decline of O<sub>2</sub> flux in the transition  
 880 from State 3 to State 4. Under the conditions of State 4, a maximum protonmotive force and high  
 881 ATP/ADP ratio are maintained. The gradual decline of  $Y_{P\gg O_2}$  towards diminishing [ADP] at State 4 must  
 882 be taken into account for calculation of P $\gg$ O<sub>2</sub> ratios (Gnaiger 2001). State 4 respiration,  $L_T$  (**Table 1**),  
 883 reflects intrinsic proton leak and ATP hydrolysis activity. O<sub>2</sub> flux in State 4 is an overestimation of  
 884 LEAK-respiration if the contaminating ATP hydrolysis activity recycles some ATP to ADP,  $J_{P\ll}$ , which  
 885 stimulates respiration coupled to phosphorylation,  $J_{P\gg} > 0$ . Some degree of mechanical disruption and  
 886 loss of mitochondrial integrity allows the exposed mitochondrial F-ATPases to hydrolyze the ATP  
 887 synthesized by the fraction of coupled mitochondria. This can be tested by inhibition of the  
 888 phosphorylation-pathway using oligomycin, ensuring that  $J_{P\gg} = 0$  (State 4o). On the other hand, the State  
 889 4 respiration reached after exhaustion of added ADP is a more physiological condition, *i.e.*, presence of  
 890 ATP, ADP and even AMP. Sequential ADP titrations re-establish State 3, followed by State 3 to State  
 891 4 transitions while sufficient O<sub>2</sub> is available. Anoxia may be reached, however, before exhaustion of  
 892 ADP (State 5).

893 **2.6.5. State 5** 'may be obtained by antimycin A treatment or by anaerobiosis' (Chance and  
 894 Williams, 1955) '. These definitions give State 5 two different meanings of ROX or anoxia, respectively.  
 895 Anoxia is obtained after exhaustion of O<sub>2</sub> in a closed respirometric chamber. Diffusion of O<sub>2</sub> from the  
 896 surroundings into the aqueous solution may be a confounding factor preventing complete anoxia  
 897 (Gnaiger 2001).

898 In **Table 3**, only States 3 and 4 are coupling control states, with the restriction that rates in State  
 899 3 may be limited kinetically by non-saturating ADP concentrations.

900

## 901 2.7. Control and regulation

902

903 The terms metabolic *control* and *regulation* are frequently used synonymously, but are  
 904 distinguished in metabolic control analysis: "We could understand the regulation as the mechanism that  
 905 occurs when a system maintains some variable constant over time, in spite of fluctuations in external  
 906 conditions (homeostasis of the internal state). On the other hand, metabolic control is the power to  
 907 change the state of the metabolism in response to an external signal" (Fell 1997). Respiratory control  
 908 may be induced by experimental control signals that exert an influence on: (1) ATP demand and ADP  
 909 phosphorylation-rate; (2) fuel substrate composition, pathway competition; (3) available amounts of  
 910 substrates and O<sub>2</sub>, *e.g.*, starvation and hypoxia; (4) the protonmotive force, redox states, flux-force  
 911 relationships, coupling and efficiency; (5) Ca<sup>2+</sup> and other ions including H<sup>+</sup>; (6) inhibitors, *e.g.*, nitric  
 912 oxide or intermediary metabolites such as oxaloacetate; (7) signalling pathways and regulatory proteins,  
 913 *e.g.*, insulin resistance, transcription factor hypoxia inducible factor 1.

914 Mechanisms of respiratory control and regulation include adjustments of: (1) enzyme activities  
 915 by allosteric mechanisms and phosphorylation; (2) enzyme content, concentrations of cofactors and  
 916 conserved moieties such as adenylates, nicotinamide adenine dinucleotide [NAD<sup>+</sup>/NADH], coenzyme  
 917 Q, cytochrome *c*; (3) metabolic channeling by supercomplexes; and (4) mitochondrial density (enzyme  
 918 concentrations and membrane area) and morphology (cristae folding, fission and fusion). Mitochondria  
 919 are targeted directly by hormones, *e.g.*, progesterone and glucacorticoids, which affect their energy  
 920 metabolism (Lee *et al.* 2013; Gerö and Szabo 2016; Price and Dai 2016; Moreno *et al.* 2017).  
 921 Evolutionary or acquired differences in the genetic and epigenetic basis of mitochondrial function (or  
 922 dysfunction) between individuals; age; biological sex, and hormone concentrations; life style including  
 923 exercise and nutrition; and environmental issues including thermal, atmospheric, toxic and  
 924 pharmacological factors, exert an influence on all control mechanisms listed above. For reviews, see  
 925 Brown 1992; Gnaiger 1993a, 2009; 2014; Paradies *et al.* 2014; Morrow *et al.* 2017.

926 Lack of control by a metabolic pathway, *e.g.*, phosphorylation-pathway, means that there will  
 927 be no response to a variable activating it, *e.g.*, [ADP]. The reverse, however, is not true as the absence  
 928 of a response to [ADP] does not exclude the phosphorylation-pathway from having some degree of  
 929 control. The degree of control of a component of the OXPHOS-pathway on an output variable, such as



930 O<sub>2</sub> flux, will in general be different from the degree of control on other outputs, such as phosphorylation-  
 931 flux or proton leak flux. Therefore, it is necessary to be specific as to which input and output are under  
 932 consideration (Fell 1997).

933 Respiratory control refers to the ability of mitochondria to adjust O<sub>2</sub> flux in response to external  
 934 control signals by engaging various mechanisms of control and regulation. Respiratory control is  
 935 monitored in a mitochondrial preparation under conditions defined as respiratory states, preferentially  
 936 under near-physiological conditions of temperature, pH, and medium ionic composition, to generate  
 937 data of higher biological relevance. When phosphorylation of ADP to ATP is stimulated or depressed,  
 938 an increase or decrease is observed in electron transfer measured as O<sub>2</sub> flux in respiratory coupling states  
 939 of intact mitochondria ('controlled states' in the classical terminology of bioenergetics). Alternatively,  
 940 coupling of electron transfer with phosphorylation is diminished by uncouplers. The corresponding  
 941 coupling control state is characterized by a high respiratory rate without control by P» (noncoupled or  
 942 'uncontrolled state').

943  
 944

### 945 3. What is a rate?

946

947 The term *rate* is not adequately defined to be useful for reporting data. Normalization of 'rates'  
 948 leads to a diversity of formats. Application of common and defined units is required for direct transfer  
 949 of reported results into a database. The second [s] is the SI unit for the base quantity *time*. It is also the  
 950 standard time-unit used in solution chemical kinetics.

951 The inconsistency of the meanings of rate becomes apparent when considering Galileo Galilei's  
 952 famous principle, that 'bodies of different weight all fall at the same rate (have a constant acceleration)'  
 953 (Coopersmith 2010). A rate may be an extensive quantity, which is a *flow*, *I*, when expressed per object  
 954 (per number of cells or organisms) or per chamber (per system). 'System' is defined as the open or  
 955 closed chamber of the measuring device. A rate is a *flux*, *J*, when expressed as a size-specific quantity  
 956 (**Figure 6A; Box 2**).

957 • **Extensive quantities:** An extensive quantity increases proportionally with system size. For  
 958 example, mass and volume are extensive quantities. Flow is an extensive quantity. The  
 959 magnitude of an extensive quantity is completely additive for non-interacting subsystems.  
 960 The magnitude of these quantities depends on the extent or size of the system (Cohen *et al.*  
 961 2008).

962 • **Size-specific quantities:** 'The adjective *specific* before the name of an extensive quantity is  
 963 often used to mean *divided by mass*' (Cohen *et al.* 2008). In this system-paradigm, mass-  
 964 specific flux is flow divided by mass of the system (the total mass of everything within the  
 965 measuring chamber or reactor). Rates are frequently expressed as volume-specific flux. A  
 966 mass-specific or volume-specific quantity is independent of the extent of non-interacting  
 967 homogenous subsystems. Tissue-specific quantities (related to the *sample* in contrast to the  
 968 *system*) are of fundamental interest in the field of comparative mitochondrial physiology,  
 969 where *specific* refers to the *type of the sample* rather than *mass of the system*. The term  
 970 *specific*, therefore, must be clarified; *sample-specific*, *e.g.*, muscle mass-specific  
 971 normalization, is distinguished from *system-specific* quantities (mass or volume; **Figure 6**).

972 • **Intensive quantities:** In contrast to size-specific properties, forces are intensive quantities  
 973 defined as the change of an extensive quantity per advancement of an energy transformation  
 974 (Gnaiger 1993b).

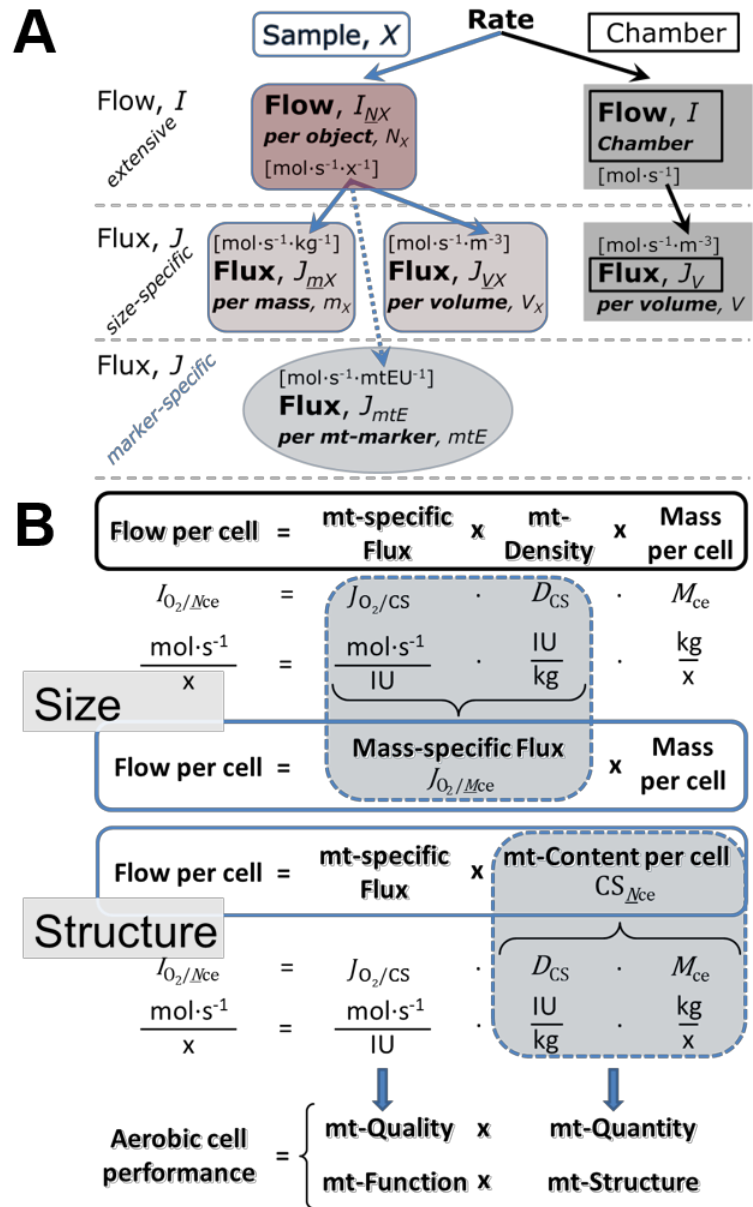
975 •  $N_X$  and  $m_X$  indicate the number format and mass format, respectively, for expressing the  
 976 quantity of a sample *X*. When different formats are indicated in symbols of derived quantities,  
 977 the format ( $\underline{N}$ ,  $\underline{m}$ ) is shown as a subscript (*underlined italic*), as in  $J_{O_2/\underline{N}X}$  and  $J_{O_2/\underline{m}X}$ . Oxygen  
 978 flow and flux are expressed in the molar format,  $n_{O_2}$  [mol], but in the volume format,  $V_{O_2}$  [m<sup>3</sup>]  
 979 in ergometry. For mass-specific flux these formats can be distinguished as  $J_{\underline{n}O_2/\underline{m}X}$  and  $J_{\underline{V}O_2/\underline{m}X}$ ,  
 980 respectively. Further examples are given in **Figure 6** and **Table 4**.

981

982 **Figure 6. Flow and flux, and**  
 983 **normalization in structure-**  
 984 **function analysis**

985 (A) When expressing metabolic  
 986 ‘rate’ measured in a chamber, a  
 987 fundamental distinction is made  
 988 between relating the rate to the  
 989 experimental sample (left) or  
 990 chamber (right). The different  
 991 meanings of rate need to be  
 992 specified by the chosen  
 993 normalization. Left: Results are  
 994 expressed as mass-specific flux,  $J_{mX}$ ,  
 995 per mg protein, dry or wet mass.  
 996 Cell volume,  $V_{ce}$ , may be used for  
 997 normalization (volume-specific  
 998 flux,  $J_{Vce}$ ). Right: Flow per chamber,  
 999  $I$ , or flux per chamber volume,  $J_V$ ,  
 1000 are merely reported for  
 1001 methodological reasons.

1002 (B)  $O_2$  flow per cell,  $I_{O_2/Nce}$ , is the  
 1003 product of mitochondria-specific  
 1004 flux, mt-density and mass per cell.  
 1005 Unstructured analysis: performance  
 1006 is the product of mass-specific flux,  
 1007  $J_{O_2/MX}$  [ $\text{mol}\cdot\text{s}^{-1}\cdot\text{kg}^{-1}$ ], and size  
 1008 (mass per cell). Structured analysis:  
 1009 performance is the product of  
 1010 mitochondrial function (mt-specific  
 1011 flux) and structure (mt-content).  
 1012 Modified from Gnaiger (2014). For  
 1013 further details see **Table 4**.



1019 **Box 2: Metabolic flows and fluxes: vectoral, vectorial, and scalar**

1020  
 1021 In a generalization of electrical terms, flow as an extensive quantity ( $I$ ; per system) is  
 1022 distinguished from flux as a size-specific quantity ( $J$ ; per system size). *Flows*,  $I_{tr}$ , are defined for all  
 1023 transformations as extensive quantities. Electric charge per unit time is electric flow or current,  $I_{el} =$   
 1024  $dQ_{el}\cdot dt^{-1}$  [ $A \equiv C\cdot s^{-1}$ ]. When dividing  $I_{el}$  by size of the system (cross-sectional area of a ‘wire’), we obtain  
 1025 flux as a size-specific quantity, which is the current density (surface-density of flow) perpendicular to  
 1026 the direction of flux,  $J_{el} = I_{el}\cdot A^{-1}$  [ $A\cdot m^{-2}$ ] (Cohen et al. 2008). Fluxes with *spatial* geometric direction and  
 1027 magnitude are *vectors*. Vector and scalar *fluxes* are related to flows as  $J_{tr} = I_{tr}\cdot A^{-1}$  [ $\text{mol}\cdot\text{s}^{-1}\cdot\text{m}^{-2}$ ] and  $J_{tr} =$   
 1028  $I_{tr}\cdot V^{-1}$  [ $\text{mol}\cdot\text{s}^{-1}\cdot\text{m}^{-3}$ ], expressing flux as an area-specific vector or volume-specific vectorial or scalar  
 1029 quantity, respectively (Gnaiger 1993b). We use the metre–kilogram–second–ampere (MKSA)  
 1030 international system of units (SI) for general cases ([m], [kg], [s] and [A]), with decimal SI prefixes for  
 1031 specific applications (**Table 4**).

1032 We suggest defining: (1) *vectoral* fluxes, which are translocations as functions of *gradients* with  
 1033 direction in geometric space in continuous systems; (2) *vectorial* fluxes, which describe translocations  
 1034 in discontinuous systems and are restricted to information on *compartmental differences*  
 1035 (transmembrane proton flux); and (3) *scalar* fluxes, which are transformations in a *homogenous* system  
 1036 (catabolic  $O_2$  flux,  $J_{kO_2}$ ).

#### 4. Normalization of rate per sample

The challenges of measuring mitochondrial respiratory flux are matched by those of normalization. Normalization (**Table 4**) is guided by physicochemical principles, methodological considerations, and conceptual strategies (**Figure 6**).

**Table 4. Sample concentrations and normalization of flux.**

Expression	Symbol	Definition	Unit	Notes
<b>Sample</b>				
identity of sample	$X$	object: cell, tissue, animal, patient		
number of sample entities $X$	$N_X$	number of objects	x	1
mass of sample $X$	$m_X$		kg	2
mass of object $X$	$M_X$	$M_X = m_X \cdot N_X^{-1}$	$\text{kg} \cdot \text{x}^{-1}$	2
<b>Mitochondria</b>				
mitochondria	mt	$X = \text{mt}$		
amount of mt-elementary components	$mtE$	quantity of mt-marker	mtEU	
<b>Concentrations</b>				
object number concentration	$C_{NX}$	$C_{NX} = N_X \cdot V^{-1}$	$\text{x} \cdot \text{m}^{-3}$	3
sample mass concentration	$C_{mX}$	$C_{mX} = m_X \cdot V^{-1}$	$\text{kg} \cdot \text{m}^{-3}$	
mitochondrial concentration	$C_{mtE}$	$C_{mtE} = mtE \cdot V^{-1}$	$\text{mtEU} \cdot \text{m}^{-3}$	4
specific mitochondrial density	$D_{mtE}$	$D_{mtE} = mtE \cdot m_X^{-1}$	$\text{mtEU} \cdot \text{kg}^{-1}$	5
mitochondrial content, $mtE$ per object $X$	$mtE_{NX}$	$mtE_{NX} = mtE \cdot N_X^{-1}$	$\text{mtEU} \cdot \text{x}^{-1}$	6
<b>O<sub>2</sub> flow and flux</b>				
flow, system	$I_{O_2}$	internal flow	$\text{mol} \cdot \text{s}^{-1}$	8
volume-specific flux	$J_{V,O_2}$	$J_{V,O_2} = I_{O_2} \cdot V^{-1}$	$\text{mol} \cdot \text{s}^{-1} \cdot \text{m}^{-3}$	9
flow per object $X$	$I_{O_2/NX}$	$I_{O_2/NX} = J_{V,O_2} \cdot C_{NX}^{-1}$	$\text{mol} \cdot \text{s}^{-1} \cdot \text{x}^{-1}$	10
mass-specific flux	$J_{O_2/mX}$	$J_{O_2/mX} = J_{V,O_2} \cdot C_{mX}^{-1}$	$\text{mol} \cdot \text{s}^{-1} \cdot \text{kg}^{-1}$	
mt-marker-specific flux	$J_{O_2/mtE}$	$J_{O_2/mtE} = J_{V,O_2} \cdot C_{mtE}^{-1}$	$\text{mol} \cdot \text{s}^{-1} \cdot \text{mtEU}^{-1}$	11

- 1045 1 The unit x for a number is not used by IUPAC. To avoid confusion, the units [ $\text{kg} \cdot \text{x}^{-1}$ ] and [kg]  
 1046 distinguish the mass per object from the mass of a sample that may contain any number of objects.  
 1047 Similarly, the units for flow per system *versus* flow per object are [ $\text{mol} \cdot \text{s}^{-1}$ ] (Note 8) and [ $\text{mol} \cdot \text{s}^{-1} \cdot \text{x}^{-1}$ ]  
 1048 (Note 10).  
 1049 2 Units are given in the MKSA system (**Box 2**). The SI prefix k is used for the SI base unit of mass (kg  
 1050 = 1,000 g). In praxis, various SI prefixes are used for convenience, to make numbers easily readable,  
 1051 e.g., 1 mg tissue, cell or mitochondrial mass instead of 0.000001 kg.  
 1052 3 In case of cells (sample  $X = \text{cells}$ ), the object number concentration is  $C_{N_{ce}} = N_{ce} \cdot V^{-1}$ , and volume  
 1053 may be expressed in [ $\text{dm}^3 \equiv \text{L}$ ] or [ $\text{cm}^3 = \text{mL}$ ]. See **Table 5** for different object types.  
 1054 4 mt-concentration is an experimental variable, dependent on sample concentration: (1)  $C_{mtE} = mtE \cdot V^{-1}$ ;  
 1055 (2)  $C_{mtE} = mtE_X \cdot C_{NX}$ ; (3)  $C_{mtE} = C_{mX} \cdot D_{mtE}$ .  
 1056 5 If the amount of mitochondria,  $mtE$ , is expressed as mitochondrial mass, then  $D_{mtE}$  is the mass  
 1057 fraction of mitochondria in the sample. If  $mtE$  is expressed as mitochondrial volume,  $V_{mt}$ , and the  
 1058 mass of sample,  $m_X$ , is replaced by volume of sample,  $V_X$ , then  $D_{mtE}$  is the volume fraction of  
 1059 mitochondria in the sample.  
 1060 6  $mtE_{NX} = mtE \cdot N_X^{-1} = C_{mtE} \cdot C_{NX}^{-1}$ .  
 1061 7 O<sub>2</sub> can be replaced by other chemicals to study different reactions, e.g., ATP, H<sub>2</sub>O<sub>2</sub>, or vesicular  
 1062 compartmental translocations, e.g., Ca<sup>2+</sup>.

- 1063 8  $I_{O_2}$  and  $V$  are defined per instrument chamber as a system of constant volume (and constant  
 1064 temperature), which may be closed or open.  $I_{O_2}$  is abbreviated for  $I_{rO_2}$ , *i.e.*, the metabolic or internal  
 1065  $O_2$  flow of the chemical reaction  $r$  in which  $O_2$  is consumed, hence the negative stoichiometric  
 1066 number,  $\nu_{O_2} = -1$ .  $I_{rO_2} = d_r n_{O_2} / dt \cdot \nu_{O_2}^{-1}$ . If  $r$  includes all chemical reactions in which  $O_2$  participates, then  
 1067  $d_r n_{O_2} = dn_{O_2} - d_e n_{O_2}$ , where  $dn_{O_2}$  is the change in the amount of  $O_2$  in the instrument chamber and  $d_e n_{O_2}$   
 1068 is the amount of  $O_2$  added externally to the system. At steady state, by definition  $dn_{O_2} = 0$ , hence  $d_r n_{O_2}$   
 1069  $= -d_e n_{O_2}$ . Note that in this context ‘external’,  $e$ , refers to the system, whereas in Figure 1 ‘external’,  
 1070  $ext$ , refers to the organism.  
 1071 9  $J_{V,O_2}$  is an experimental variable, expressed per volume of the instrument chamber.  
 1072 10  $I_{O_2/NX}$  is a physiological variable, depending on the size of entity  $X$ .  
 1073 11 There are many ways to normalize for a mitochondrial marker, that are used in different experimental  
 1074 approaches: (1)  $J_{O_2/mtE} = J_{V,O_2} \cdot C_{mtE}^{-1}$ ; (2)  $J_{O_2/mtE} = J_{V,O_2} \cdot C_{mX}^{-1} \cdot D_{mtE}^{-1} = J_{O_2/mX} \cdot D_{mtE}^{-1}$ ; (3)  $J_{O_2/mtE} =$   
 1075  $J_{V,O_2} \cdot C_{NX}^{-1} \cdot mtE_{NX}^{-1} = I_{O_2/NX} \cdot mtE_{NX}^{-1}$ ; (4)  $J_{O_2/mtE} = I_{O_2} \cdot mtE^{-1}$ . The mt-elementary unit [mtEU] varies depending  
 1076 on the mt-marker.  
 1077  
 1078  
 1079

**Table 5. Sample types, X, abbreviations, and quantification.**

Identity of sample	$X$	$N_X$	Mass <sup>a</sup>	Volume	mt-Marker
mitochondrial preparation		[x]	[kg]	[m <sup>3</sup> ]	[mtEU]
isolated mitochondria	imt		$m_{mt}$	$V_{mt}$	$mtE$
tissue homogenate	thom		$m_{thom}$		$mtE_{thom}$
permeabilized tissue	pti		$m_{pti}$		$mtE_{pti}$
permeabilized fibre	pfi		$m_{pfi}$		$mtE_{pfi}$
permeabilized cell	pce	$N_{pce}$	$M_{pce}$	$V_{pce}$	$mtE_{pce}$
cells <sup>b</sup>	ce	$N_{ce}$	$M_{ce}$	$V_{ce}$	$mtE_{ce}$
intact cell, viable cell	vce	$N_{vce}$	$M_{vce}$	$V_{vce}$	
dead cell	dce	$N_{dce}$	$M_{dce}$	$V_{dce}$	
organism	org	$N_{org}$	$M_{org}$	$V_{org}$	

<sup>a</sup> Instead of mass, the wet weight or dry weight is frequently stated,  $W_w$  or  $W_d$ .  $m_X$  is mass of the sample [kg],  $M_X$  is mass of the object [kg·x<sup>-1</sup>] (Table 4).

<sup>b</sup> Total cell count,  $N_{ce} = N_{vce} + N_{dce}$

#### 4.1. Flow: per object

**4.1.1. Number concentration,  $C_{NX}$ :** Normalization per sample concentration is routinely required to report respiratory data.  $C_{NX}$  is the experimental number concentration of sample  $X$ . In the case of animals, *e.g.*, nematodes,  $C_{NX} = N_X/V$  [x·L<sup>-1</sup>], where  $N_X$  is the number of organisms in the chamber. Similarly, the number of cells per chamber volume is the number concentration of permeabilized or intact cells  $C_{Nce} = N_{ce}/V$  [x·L<sup>-1</sup>], where  $N_{ce}$  is the number of cells in the chamber (Table 4).

**4.1.2. Flow per object,  $I_{O_2/NX}$ :**  $O_2$  flow per cell is calculated from volume-specific  $O_2$  flux,  $J_{V,O_2}$  [nmol·s<sup>-1</sup>·L<sup>-1</sup>] (per  $V$  of the measurement chamber [L]), divided by the number concentration of cells. The total cell count is the sum of viable and dead cells,  $N_{ce} = N_{vce} + N_{dce}$  (Table 5). The cell viability index,  $VI = N_{vce}/N_{ce}$ , is the ratio of viable cells ( $N_{vce}$ ; before experimental permeabilization) per total cell count. After experimental permeabilization, all cells are permeabilized,  $N_{pce} = N_{ce}$ . The cell viability index can be used to normalize respiration for the number of cells that have been viable before experimental permeabilization,  $I_{O_2/Nvce} = I_{O_2/Nce}/VI$ , considering that mitochondrial respiratory dysfunction in dead cells should be eliminated as a confounding factor.

The complexity changes when the object is a whole organism studied as an experimental model. The scaling law in respiratory physiology reveals a strong interaction between  $O_2$  flow and individual body mass: *basal* metabolic rate (flow) does not increase linearly with body mass, whereas *maximum* mass-specific  $O_2$  flux,  $\dot{V}_{O_2max}$  or  $\dot{V}_{O_2peak}$ , is approximately constant across a large range of individual body mass (Weibel and Hoppeler 2005). Individuals, breeds and species, however, deviate substantially from this relationship.  $\dot{V}_{O_2peak}$  of human endurance athletes is 60 to 80 mL  $O_2$ ·min<sup>-1</sup>·kg<sup>-1</sup> body mass, converted to  $J_{O_2peak/Morg}$  of 45 to 60 nmol·s<sup>-1</sup>·g<sup>-1</sup> (Gnaiger 2014; Table 6).



#### 4.2. Size-specific flux: per sample size

**4.2.1. Sample concentration,  $C_{mX}$ :** Considering permeabilized tissue, homogenate or cells as the sample,  $X$ , the sample mass is  $m_X$  [mg], which is frequently measured as wet or dry weight,  $W_w$  or  $W_d$  [mg], respectively, or as amount of protein,  $m_{\text{protein}}$ . The sample concentration is the mass of the subsample per volume of the measurement chamber,  $C_{mX} = m_X/V$  [ $\text{g}\cdot\text{L}^{-1} = \text{mg}\cdot\text{mL}^{-1}$ ].  $X$  is the type of sample—isolated mitochondria, tissue homogenate, permeabilized fibres or cells (**Table 5**).

**4.2.2. Size-specific flux:** Cellular  $\text{O}_2$  flow can be compared between cells of identical size. To take into account changes and differences in cell size, normalization is required to obtain cell size-specific or mitochondrial marker-specific  $\text{O}_2$  flux (Renner *et al.* 2003).

- **Mass-specific flux,  $J_{\text{O}_2/mX}$  [ $\text{mol}\cdot\text{s}^{-1}\cdot\text{kg}^{-1}$ ]:** Mass-specific flux is obtained by expressing respiration per mass of sample,  $m_X$  [mg]. Flow per cell is divided by mass per cell,  $J_{\text{O}_2/mce} = I_{\text{O}_2/Nce}/M_{Nce}$ . Or chamber volume-specific flux,  $J_{V,\text{O}_2}$ , is divided by mass concentration of  $X$  in the chamber,  $J_{\text{O}_2/mX} = J_{V,\text{O}_2}/C_{mX}$ .
- **Cell volume-specific flux,  $J_{\text{O}_2/VX}$  [ $\text{mol}\cdot\text{s}^{-1}\cdot\text{m}^{-3}$ ]:** Sample volume-specific flux is obtained by expressing respiration per volume of sample. For example, in the case of using cells as sample will be the volume of cells added to the chamber (**Figure 6**).

If size-specific  $\text{O}_2$  flux is constant and independent of sample size, then there is no interaction between the subsystems. For example, a 1.5 mg and a 3.0 mg muscle sample respire at identical mass-specific flux. Mass-specific  $\text{O}_2$  flux, however, may change with the mass of a tissue sample, cells or isolated mitochondria in the measuring chamber, in which the nature of the interaction becomes an issue. Therefore, cell density must be optimized, particularly in experiments carried out in wells, considering the confluency of the cell monolayer or clumps of cells (Salabei *et al.* 2014).

#### 4.3. Marker-specific flux: per mitochondrial content

Tissues can contain multiple cell populations that may have distinct mitochondrial subtypes. Mitochondria undergo dynamic fission and fusion cycles, and can exist in multiple stages and sizes that may be altered by a range of factors. The isolation of mitochondria (often achieved through differential centrifugation) can therefore yield a subsample of the mitochondrial types present in a tissue, depending on the isolation protocols utilized, *e.g.*, centrifugation speed. This possible bias should be taken into account when planning experiments using isolated mitochondria. Different sizes of mitochondria are enriched at specific centrifugation speeds, which can be used strategically for isolation of mitochondrial subpopulations.

Part of the mitochondrial content of a tissue is lost during preparation of isolated mitochondria. The fraction of isolated mitochondria obtained from a tissue sample is expressed as mitochondrial recovery. At a high mitochondrial recovery, the fraction of isolated mitochondria is more representative of the total mitochondrial population than in preparations characterized by low recovery. Determination of the mitochondrial recovery and yield is based on measurement of the concentration of a mitochondrial marker in the stock of isolated mitochondria,  $C_{mtE,\text{stock}}$ , and crude tissue homogenate,  $C_{mtE,\text{thom}}$ , which simultaneously provides information on the specific mitochondrial density in the sample,  $D_{mtE}$  (**Table 4**).

When discussing concepts of normalization, it is essential to consider the question posed by the study. If the study aims at comparing tissue performance—such as the effects of a treatment on a specific tissue, then normalization for tissue mass or protein content is appropriate. However, if the aim is to find differences in mitochondrial function independent of mitochondrial density (**Table 4**), then normalization to a mitochondrial marker is imperative (**Figure 6**). One cannot assume that quantitative changes in various markers—such as mitochondrial proteins—necessarily occur in parallel with one another. It should be established that the marker chosen is not selectively altered by the performed treatment. In conclusion, the normalization must reflect the question under investigation to reach a satisfying answer. On the other hand, the goal of comparing results across projects and institutions requires standardization on normalization for entry into a databank.

**4.3.1. Mitochondrial concentration,  $C_{mtE}$ , and mitochondrial markers:** Mitochondrial organelles compose a dynamic cellular reticulum in various states of fusion and fission. Hence, the definition of an ‘amount’ of mitochondria is often misconceived: mitochondria cannot be counted reliably as a number of occurring elementary components. Therefore, quantification of the amount of

1162 mitochondria depends on the measurement of chosen mitochondrial markers. “Mitochondria are the  
 1163 structural and functional elementary units of cell respiration” (Gnaiger 2014). The quantity of a  
 1164 mitochondrial marker can reflect the amount of *mitochondrial elementary components*,  $mtE$ , expressed  
 1165 in various mitochondrial elementary units [mtEU] specific for each measured mt-marker (**Table 4**).  
 1166 However, since mitochondrial quality may change in response to stimuli—particularly in mitochondrial  
 1167 dysfunction (Campos *et al.* 2017) and after exercise training (Pesta *et al.* 2011) and during aging (Daum  
 1168 *et al.* 2013)—some markers can vary while others are unchanged: (1) Mitochondrial volume and  
 1169 membrane area are structural markers, whereas mitochondrial protein mass is commonly used as a  
 1170 marker for isolated mitochondria. (2) Molecular and enzymatic mitochondrial markers (amounts or  
 1171 activities) can be selected as matrix markers, *e.g.*, citrate synthase activity, mtDNA; mtIM-markers, *e.g.*,  
 1172 cytochrome *c* oxidase activity,  $aa_3$  content, cardiolipin, or mtOM-markers, *e.g.*, the voltage-dependent  
 1173 anion channel (VDAC), TOM20. (3) Extending the measurement of mitochondrial marker enzyme  
 1174 activity to mitochondrial pathway capacity, ET- or OXPHOS-capacity can be considered as an  
 1175 integrative functional mitochondrial marker.

1176 Depending on the type of mitochondrial marker, the mitochondrial elementary component,  $mtE$ ,  
 1177 is expressed in marker-specific units. Mitochondrial concentration in the measurement chamber and the  
 1178 tissue of origin are quantified as (1) a quantity for normalization in functional analyses,  $C_{mtE}$ , and (2) a  
 1179 physiological output that is the result of mitochondrial biogenesis and degradation,  $D_{mtE}$ , respectively  
 1180 (**Table 4**). It is recommended, therefore, to distinguish *experimental mitochondrial concentration*,  $C_{mtE}$   
 1181  $= mtE/V$  and *physiological mitochondrial density*,  $D_{mtE} = mtE/m_X$ . Then mitochondrial density is the  
 1182 amount of mitochondrial elementary components per mass of tissue, which is a biological variable  
 1183 (**Figure 6**). The experimental variable is mitochondrial density multiplied by sample mass concentration  
 1184 in the measuring chamber,  $C_{mtE} = D_{mtE} \cdot C_{m_X}$ , or mitochondrial content multiplied by sample number  
 1185 concentration,  $C_{mtE} = mtE_X \cdot C_{N_X}$  (**Table 4**).

1186 **4.3.2. mt-Marker-specific flux,  $J_{O_2/mtE}$ :** Volume-specific metabolic  $O_2$  flux depends on: (1) the  
 1187 sample concentration in the volume of the instrument chamber,  $C_{m_X}$ , or  $C_{N_X}$ ; (2) the mitochondrial  
 1188 density in the sample,  $D_{mtE} = mtE/m_X$  or  $mtE_X = mtE/N_X$ ; and (3) the specific mitochondrial activity or  
 1189 performance per elementary mitochondrial unit,  $J_{O_2/mtE} = J_{V,O_2}/C_{mtE}$  [ $\text{mol} \cdot \text{s}^{-1} \cdot \text{mtEU}^{-1}$ ] (**Table 4**).  
 1190 Obviously, the numerical results for  $J_{O_2/mtE}$  vary with the type of mitochondrial marker chosen for  
 1191 measurement of  $mtE$  and  $C_{mtE} = mtE/V$  [ $\text{mtEU} \cdot \text{m}^{-3}$ ].

1192 Different methods are involved in the quantification of mitochondrial markers and have different  
 1193 strengths. Some problems are common for all mitochondrial markers,  $mtE$ : (1) Accuracy of  
 1194 measurement is crucial, since even a highly accurate and reproducible measurement of  $O_2$  flux results  
 1195 in an inaccurate and noisy expression if normalized by a biased and noisy measurement of a  
 1196 mitochondrial marker. This problem is acute in mitochondrial respiration because the denominators used  
 1197 (the mitochondrial markers) are often small moieties of which accurate and precise determination is  
 1198 difficult. This problem can be avoided when  $O_2$  fluxes measured in substrate-uncoupler-inhibitor  
 1199 titration protocols are normalized for flux in a defined respiratory reference state, which is used as an  
 1200 *internal* marker and yields flux control ratios, *FCRs*. *FCRs* are independent of externally measured  
 1201 markers and, therefore, are statistically robust, considering the limitations of ratios in general (Jasienski  
 1202 and Bazzaz 1999). *FCRs* indicate qualitative changes of mitochondrial respiratory control, with highest  
 1203 quantitative resolution, separating the effect of mitochondrial density or concentration on  $J_{O_2/m_X}$  and  
 1204  $I_{O_2/N_X}$  from that of function per elementary mitochondrial marker,  $J_{O_2/mtE}$  (Pesta *et al.* 2011; Gnaiger  
 1205 2014). (2) If mitochondrial quality does not change and only the amount of mitochondria varies as a  
 1206 determinant of mass-specific flux, any marker is equally qualified in principle; then in practice selection  
 1207 of the optimum marker depends only on the accuracy and precision of measurement of the mitochondrial  
 1208 marker. (3) If mitochondrial flux control ratios change, then there may not be any best mitochondrial  
 1209 marker. In general, measurement of multiple mitochondrial markers enables a comparison and  
 1210 evaluation of normalization for these mitochondrial markers. Particularly during postnatal development,  
 1211 the activity of marker enzymes—such as cytochrome *c* oxidase and citrate synthase—follows different  
 1212 time courses (Drahota *et al.* 2004). Evaluation of mitochondrial markers in healthy controls is  
 1213 insufficient for providing guidelines for application in the diagnosis of pathological states and specific  
 1214 treatments.

1215 In line with the concept of the respiratory control ratio (Chance and Williams 1955a), the most  
 1216 readily used normalization is that of flux control ratios and flux control factors (Gnaiger 2014). Selection  
 1217 of the state of maximum flux in a protocol as the reference state has the advantages of: (1) internal

1218 normalization; (2) statistically validated linearization of the response in the range of 0 to 1; and (3)  
 1219 consideration of maximum flux for integrating a large number of elementary steps in the OXPHOS- or  
 1220 ET-pathways. This reduces the risk of selecting a functional marker that is specifically altered by the  
 1221 treatment or pathology, yet increases the chance that the highly integrative pathway is disproportionately  
 1222 affected, *e.g.*, the OXPHOS- rather than ET-pathway in case of an enzymatic defect in the  
 1223 phosphorylation-pathway. In this case, additional information can be obtained by reporting flux control  
 1224 ratios based on a reference state that indicates stable tissue-mass specific flux.

1225 Stereological determination of mitochondrial content via two-dimensional transmission electron  
 1226 microscopy can have limitations due to the dynamics of mitochondrial size (Meinild Lundby *et al.*  
 1227 2017). Accurate determination of three-dimensional volume by two-dimensional microscopy can be  
 1228 both time consuming and statistically challenging (Larsen *et al.* 2012).

1229 The validity of using mitochondrial marker enzymes (citrate synthase activity, CI to CIV amount  
 1230 or activity) for normalization of flux is limited in part by the same factors that apply to flux control  
 1231 ratios. Strong correlations between various mitochondrial markers and citrate synthase activity  
 1232 (Reichmann *et al.* 1985; Boushel *et al.* 2007; Mogensen *et al.* 2007) are expected in a specific tissue of  
 1233 healthy persons and in disease states not specifically targeting citrate synthase. Citrate synthase activity  
 1234 is acutely modifiable by exercise (Tonkonogi *et al.* 1997; Leek *et al.* 2001). Evaluation of mitochondrial  
 1235 markers related to a selected age and sex cohort cannot be extrapolated to provide recommendations for  
 1236 normalization in respirometric diagnosis of disease, in different states of development and ageing,  
 1237 different cell types, tissues, and species. mtDNA normalized to nDNA via qPCR is correlated to  
 1238 functional mitochondrial markers including OXPHOS- and ET-capacity in some cases (Puntschart *et al.*  
 1239 1995; Wang *et al.* 1999; Menshikova *et al.* 2006; Boushel *et al.* 2007; Ehinger *et al.* 2015), but lack of  
 1240 such correlations have been reported (Menshikova *et al.* 2005; Schultz and Wiesner 2000; Pesta *et al.*  
 1241 2011). Several studies indicate a strong correlation between cardiolipin content and increase in  
 1242 mitochondrial function with exercise (Menshikova *et al.* 2005; Menshikova *et al.* 2007; Larsen *et al.*  
 1243 2012; Faber *et al.* 2014), but it has not been evaluated as a general mitochondrial biomarker in disease.  
 1244 With no single best mitochondrial marker, a good strategy is to quantify several different biomarkers to  
 1245 minimize the decorrelating effects caused by diseases, treatments, or other factors. Determination of  
 1246 multiple markers, particularly a matrix marker and a marker from the mtIM, allows tracking changes in  
 1247 mitochondrial quality defined by their ratio.

## 1250 5. Normalization of rate per system

### 1252 5.1. Flow: per chamber

1254 The experimental system (experimental chamber) is part of the measurement instrument,  
 1255 separated from the environment as an isolated, closed, open, isothermal or non-isothermal system  
 1256 (Table 4). Reporting O<sub>2</sub> flows per respiratory chamber,  $I_{O_2}$  [nmol·s<sup>-1</sup>], restricts the analysis to intra-  
 1257 experimental comparison of relative differences.

### 1259 5.2. Flux: per chamber volume

1261 **5.2.1. System-specific flux,  $J_{V,O_2}$ :** We distinguish between (1) the *system* with volume  $V$  and mass  
 1262  $m$  defined by the system boundaries, and (2) the *sample* or *objects* with volume  $V_X$  and mass  $m_X$  that are  
 1263 enclosed in the experimental chamber (Figure 6). Metabolic O<sub>2</sub> flow per object,  $I_{O_2/N_X}$ , is the total O<sub>2</sub>  
 1264 flow in the system divided by the number of objects,  $N_X$ , in the system.  $I_{O_2/N_X}$  increases as the mass of  
 1265 the object is increased. Sample mass-specific O<sub>2</sub> flux,  $J_{O_2/m_X}$  should be independent of the mass of the  
 1266 sample studied in the instrument chamber, but system volume-specific O<sub>2</sub> flux,  $J_{V,O_2}$  (per volume of the  
 1267 instrument chamber), increases in proportion to the mass of the sample in the chamber. Although  $J_{V,O_2}$   
 1268 depends on mass-concentration of the sample in the chamber, it should be independent of the chamber  
 1269 (system) volume at constant sample mass-concentration. There are practical limitations to increasing the  
 1270 mass-concentration of the sample in the chamber, when one is concerned about crowding effects and  
 1271 instrumental time resolution.

1272 **5.2.2. Advancement per volume:** When the reactor volume does not change during the reaction,  
 1273 which is typical for liquid phase reactions, the volume-specific flux of a chemical reaction  $r$  is the time

1274 derivative of the advancement of the reaction per unit volume,  $J_{V,rB} = d_r \xi_B / dt \cdot V^{-1}$  [(mol·s<sup>-1</sup>)·L<sup>-1</sup>]. The *rate*  
 1275 *of concentration change* is  $dc_B/dt$  [(mol·L<sup>-1</sup>)·s<sup>-1</sup>], where concentration is  $c_B = n_B/V$ . There is a difference  
 1276 between (1)  $J_{V,rO_2}$  [mol·s<sup>-1</sup>·L<sup>-1</sup>] and (2) rate of concentration change [mol·L<sup>-1</sup>·s<sup>-1</sup>]. These merge into a  
 1277 single expression only in closed systems. In open systems, internal transformations (catabolic flux, O<sub>2</sub>  
 1278 consumption) are distinguished from external flux (such as O<sub>2</sub> supply). External fluxes of all substances  
 1279 are zero in closed systems. In a closed chamber O<sub>2</sub> consumption (internal flux of catabolic reactions  $k$ ;  
 1280  $I_{kO_2}$  [pmol·s<sup>-1</sup>]) causes a decline in the amount of O<sub>2</sub> in the system,  $n_{O_2}$  [nmol]. Normalization of these  
 1281 quantities for the volume of the system,  $V$  [L  $\equiv$  dm<sup>3</sup>], yields volume-specific O<sub>2</sub> flux,  $J_{V,kO_2} = I_{kO_2}/V$   
 1282 [nmol·s<sup>-1</sup>·L<sup>-1</sup>], and O<sub>2</sub> concentration, [O<sub>2</sub>] or  $c_{O_2} = n_{O_2}/V$  [ $\mu$ mol·L<sup>-1</sup> =  $\mu$ M = nmol·mL<sup>-1</sup>]. Instrumental  
 1283 background O<sub>2</sub> flux is due to external flux into a non-ideal closed respirometer, so total volume-specific  
 1284 flux has to be corrected for instrumental background O<sub>2</sub> flux—O<sub>2</sub> diffusion into or out of the  
 1285 instrumental chamber.  $J_{V,kO_2}$  is relevant mainly for methodological reasons and should be compared with  
 1286 the accuracy of instrumental resolution of background-corrected flux, *e.g.*,  $\pm 1$  nmol·s<sup>-1</sup>·L<sup>-1</sup> (Gnaiger  
 1287 2001). ‘Catabolic’ indicates O<sub>2</sub> flux,  $J_{kO_2}$ , corrected for: (1) instrumental background O<sub>2</sub> flux; (2)  
 1288 chemical background O<sub>2</sub> flux due to autoxidation of chemical components added to the incubation  
 1289 medium; and (3) *Rox* for O<sub>2</sub>-consuming side reactions unrelated to the catabolic pathway  $k$ .

1290  
1291

## 1292 6. Conversion of units

1293

1294 Many different units have been used to report the O<sub>2</sub> consumption rate, OCR (Table 6). SI base  
 1295 units provide the common reference to introduce the theoretical principles (Figure 6), and are used with  
 1296 appropriately chosen SI prefixes to express numerical data in the most practical format, with an effort  
 1297 towards unification within specific areas of application (Table 7). Reporting data in SI units—including  
 1298 the mole [mol], coulomb [C], joule [J], and second [s]—should be encouraged, particularly by journals  
 1299 that propose the use of SI units.

1300

1301 **Table 6. Conversion of various formats and units used in respirometry and**  
 1302 **ergometry.**  $e^-$  is the number of electrons or reducing equivalents.  $z_B$  is the charge number  
 1303 of entity B.  
 1304

Format	1 Unit		Multiplication factor	SI-unit	Notes
$\underline{n}$	ng.atom O·s <sup>-1</sup>	(2 $e^-$ )	0.5	nmol O <sub>2</sub> ·s <sup>-1</sup>	
$\underline{n}$	ng.atom O·min <sup>-1</sup>	(2 $e^-$ )	8.33	pmol O <sub>2</sub> ·s <sup>-1</sup>	
$\underline{n}$	natom O·min <sup>-1</sup>	(2 $e^-$ )	8.33	pmol O <sub>2</sub> ·s <sup>-1</sup>	
$\underline{n}$	nmol O <sub>2</sub> ·min <sup>-1</sup>	(4 $e^-$ )	16.67	pmol O <sub>2</sub> ·s <sup>-1</sup>	
$\underline{n}$	nmol O <sub>2</sub> ·h <sup>-1</sup>	(4 $e^-$ )	0.2778	pmol O <sub>2</sub> ·s <sup>-1</sup>	
$\underline{V}$ to $\underline{n}$	mL O <sub>2</sub> ·min <sup>-1</sup> at STPD <sup>a</sup>		0.744	$\mu$ mol O <sub>2</sub> ·s <sup>-1</sup>	1
$\underline{e}$ to $\underline{n}$	W = J/s at -470 kJ/mol O <sub>2</sub>		-2.128	$\mu$ mol O <sub>2</sub> ·s <sup>-1</sup>	
$\underline{e}$ to $\underline{n}$	mA = mC·s <sup>-1</sup>	( $z_{H^+} = 1$ )	10.36	nmol H <sup>+</sup> ·s <sup>-1</sup>	2
$\underline{e}$ to $\underline{n}$	mA = mC·s <sup>-1</sup>	( $z_{O_2} = 4$ )	2.59	nmol O <sub>2</sub> ·s <sup>-1</sup>	2
$\underline{n}$ to $\underline{e}$	nmol H <sup>+</sup> ·s <sup>-1</sup>	( $z_{H^+} = 1$ )	0.09649	mA	3
$\underline{n}$ to $\underline{e}$	nmol O <sub>2</sub> ·s <sup>-1</sup>	( $z_{O_2} = 4$ )	0.38594	mA	3

1305 1 At standard temperature and pressure dry (STPD: 0 °C = 273.15 K and 1 atm = 101.325 kPa =  
 1306 760 mmHg), the molar volume of an ideal gas,  $V_m$ , and  $V_{m,O_2}$  is 22.414 and 22.392 L·mol<sup>-1</sup>,  
 1307 respectively. Rounded to three decimal places, both values yield the conversion factor of 0.744.  
 1308 For comparison at normal temperature and pressure dry (NTPD: 20 °C),  $V_{m,O_2}$  is 24.038 L·mol<sup>-1</sup>.  
 1309 Note that the SI standard pressure is 100 kPa.

1310 2 The multiplication factor is  $10^6/(z_B \cdot F)$ .

1311 3 The multiplication factor is  $z_B \cdot F/10^6$ .

1312



1313 **Table 7. Conversion of units with preservation of numerical values.**

Name	Frequently used unit	Equivalent unit	Notes
volume-specific flux, $J_{V,O_2}$	$\text{pmol}\cdot\text{s}^{-1}\cdot\text{mL}^{-1}$	$\text{nmol}\cdot\text{s}^{-1}\cdot\text{L}^{-1}$	1
cell-specific flow, $I_{O_2/\text{cell}}$	$\text{mmol}\cdot\text{s}^{-1}\cdot\text{L}^{-1}$	$\text{mol}\cdot\text{s}^{-1}\cdot\text{m}^{-3}$	
	$\text{pmol}\cdot\text{s}^{-1}\cdot 10^{-6}$ cells	$\text{amol}\cdot\text{s}^{-1}\cdot\text{cell}^{-1}$	2
cell number concentration, $C_{Nce}$	$\text{pmol}\cdot\text{s}^{-1}\cdot 10^{-9}$ cells	$\text{zmol}\cdot\text{s}^{-1}\cdot\text{cell}^{-1}$	3
	$10^6$ cells $\cdot\text{mL}^{-1}$	$10^9$ cells $\cdot\text{L}^{-1}$	
mitochondrial protein concentration, $C_{mtE}$	$0.1$ mg $\cdot\text{mL}^{-1}$	$0.1$ g $\cdot\text{L}^{-1}$	
mass-specific flux, $J_{O_2/m}$	$\text{pmol}\cdot\text{s}^{-1}\cdot\text{mg}^{-1}$	$\text{nmol}\cdot\text{s}^{-1}\cdot\text{g}^{-1}$	4
catabolic power, $P_k$	$\mu\text{W}\cdot 10^{-6}$ cells	$\text{pW}\cdot\text{cell}^{-1}$	1
volume	1,000 L	$\text{m}^3$ (1,000 kg)	
	L	$\text{dm}^3$ (kg)	
	mL	$\text{cm}^3$ (g)	
	$\mu\text{L}$	$\text{mm}^3$ (mg)	
	fL	$\mu\text{m}^3$ (pg)	5
amount of substance concentration	$\text{M} = \text{mol}\cdot\text{L}^{-1}$	$\text{mol}\cdot\text{dm}^{-3}$	

1314 1 pmol: picomole =  $10^{-12}$  mol1315 2 amol: attomole =  $10^{-18}$  mol1316 3 zmol: zeptomole =  $10^{-21}$  mol

1317

1318 Although volume is expressed as  $\text{m}^3$  using the SI base unit, the litre [ $\text{dm}^3$ ] is a conventional unit  
 1319 of volume for concentration and is used for most solution chemical kinetics. If one multiplies  $I_{O_2/Nce}$  by  
 1320  $C_{Nce}$ , then the result will not only be the amount of  $\text{O}_2$  [mol] consumed per time [ $\text{s}^{-1}$ ] in one litre [ $\text{L}^{-1}$ ],  
 1321 but also the change in  $\text{O}_2$  concentration per second (for any volume of an ideally closed system). This  
 1322 is ideal for kinetic modeling as it blends with chemical rate equations where concentrations are typically  
 1323 expressed in  $\text{mol}\cdot\text{L}^{-1}$  (Wagner *et al.* 2011). In studies of multinuclear cells—such as differentiated  
 1324 skeletal muscle cells—it is easy to determine the number of nuclei but not the total number of cells. A  
 1325 generalized concept, therefore, is obtained by substituting cells by nuclei as the sample entity. This does  
 1326 not hold, however, for non-nucleated platelets.

1327 For studies of cells, we recommend that respiration be expressed, as far as possible, as: (1)  $\text{O}_2$   
 1328 flux normalized for a mitochondrial marker, for separation of the effects of mitochondrial quality and  
 1329 content on cell respiration (this includes  $FCRs$  as a normalization for a functional mitochondrial  
 1330 marker); (2)  $\text{O}_2$  flux in units of cell volume or mass, for comparison of respiration of cells with different  
 1331 cell size (Renner *et al.* 2003) and with studies on tissue preparations, and (3)  $\text{O}_2$  flow in units of attomole  
 1332 ( $10^{-18}$  mol) of  $\text{O}_2$  consumed per second by each cell [ $\text{amol}\cdot\text{s}^{-1}\cdot\text{cell}^{-1}$ ], numerically equivalent to  
 1333 [ $\text{pmol}\cdot\text{s}^{-1}\cdot 10^{-6}$  cells]. This convention allows information to be easily used when designing experiments  
 1334 in which  $\text{O}_2$  flow must be considered. For example, to estimate the volume-specific  $\text{O}_2$  flux in an  
 1335 instrument chamber that would be expected at a particular cell number concentration, one simply needs  
 1336 to multiply the flow per cell by the number of cells per volume of interest. This provides the amount of  
 1337  $\text{O}_2$  [mol] consumed per time [ $\text{s}^{-1}$ ] per unit volume [ $\text{L}^{-1}$ ]. At an  $\text{O}_2$  flow of  $100$   $\text{amol}\cdot\text{s}^{-1}\cdot\text{cell}^{-1}$  and a cell  
 1338 density of  $10^9$  cells $\cdot\text{L}^{-1}$  ( $10^6$  cells $\cdot\text{mL}^{-1}$ ), the volume-specific  $\text{O}_2$  flux is  $100$   $\text{nmol}\cdot\text{s}^{-1}\cdot\text{L}^{-1}$  ( $100$   
 1339  $\text{pmol}\cdot\text{s}^{-1}\cdot\text{mL}^{-1}$ ).

1340 ET-capacity in human cell types including HEK 293, primary HUVEC, and fibroblasts ranges  
 1341 from  $50$  to  $180$   $\text{amol}\cdot\text{s}^{-1}\cdot\text{cell}^{-1}$ , measured in intact cells in the noncoupled state (see Gnaiger 2014). At  
 1342  $100$   $\text{amol}\cdot\text{s}^{-1}\cdot\text{cell}^{-1}$  corrected for  $Rox$ , the current across the mt-membranes,  $I_{H^+e}$ , approximates  $193$   
 1343  $\text{pA}\cdot\text{cell}^{-1}$  or  $0.2$  nA per cell. See Rich (2003) for an extension of quantitative bioenergetics from the  
 1344 molecular to the human scale, with a transmembrane proton flux equivalent to  $520$  A in an adult at a  
 1345 catabolic power of  $-110$  W. Modelling approaches illustrate the link between protonmotive force and  
 1346 currents (Willis *et al.* 2016).

1347 We consider isolated mitochondria as powerhouses and proton pumps as molecular machines to  
 1348 relate experimental results to energy metabolism of the intact cell. The cellular  $P_{\gg}/\text{O}_2$  based on oxidation

of glycogen is increased by the glycolytic (fermentative) substrate-level phosphorylation of 3 P $\gg$ /Glyc or 0.5 mol P $\gg$  for each mol O<sub>2</sub> consumed in the complete oxidation of a mol glycosyl unit (Glyc). Adding 0.5 to the mitochondrial P $\gg$ /O<sub>2</sub> ratio of 5.4 yields a bioenergetic cell physiological P $\gg$ /O<sub>2</sub> ratio close to 6. Two NADH equivalents are formed during glycolysis and transported from the cytosol into the mitochondrial matrix, either by the malate-aspartate shuttle or by the glycerophosphate shuttle (**Figure 2A**) resulting in different theoretical yields of ATP generated by mitochondria, the energetic cost of which potentially must be taken into account. Considering also substrate-level phosphorylation in the TCA cycle, this high P $\gg$ /O<sub>2</sub> ratio not only reflects proton translocation and OXPHOS studied in isolation, but integrates mitochondrial physiology with energy transformation in the living cell (Gnaiger 1993a).

## 7. Conclusions

Catabolic cell respiration is the process of exergonic and exothermic energy transformation in which scalar redox reactions are coupled to vectorial ion translocation across a semipermeable membrane, which separates the small volume of a bacterial cell or mitochondrion from the larger volume of its surroundings. The electrochemical exergy can be partially conserved in the phosphorylation of ADP to ATP or in ion pumping, or dissipated in an electrochemical short-circuit. Respiration is thus clearly distinguished from fermentation as the counterpart of cellular core energy metabolism. An O<sub>2</sub> flux balance scheme illustrates the relationships and general definitions (**Figures 1 and 2**).

---

### Box 3: Recommendations for studies with mitochondrial preparations

- Normalization of respiratory rates should be provided as far as possible:
  1. *Biophysical normalization*: on a per cell basis as O<sub>2</sub> flow; this may not be possible when dealing with coenocytic organisms, *e.g.*, filamentous fungi, or tissues without cross-walls separating individual cells, *e.g.*, muscle fibers.
  2. *Cellular normalization*: per g protein; per cell- or tissue-mass as mass-specific O<sub>2</sub> flux; per cell volume as cell volume-specific flux.
  3. *Mitochondrial normalization*: per mitochondrial marker as mt-specific flux.
- With information on cell size and the use of multiple normalizations, maximum potential information is available (Renner *et al.* 2003; Wagner *et al.* 2011; Gnaiger 2014). Reporting flow in a respiratory chamber [nmol·s<sup>-1</sup>] is discouraged, since it restricts the analysis to intra-experimental comparison of relative (qualitative) differences.
- Catabolic mitochondrial respiration is distinguished from residual O<sub>2</sub> consumption. Fluxes in mitochondrial coupling states should be, as far as possible, corrected for residual O<sub>2</sub> consumption.
- Different mechanisms of uncoupling should be distinguished by defined terms. The tightness of coupling relates to these uncoupling mechanisms, whereas the coupling stoichiometry varies as a function the substrate type involved in ET-pathways with either three or two redox proton pumps operating in series. Separation of tightness of coupling from the pathway-dependent coupling stoichiometry is possible only when the substrate type undergoing oxidation remains the same for respiration in LEAK-, OXPHOS-, and ET-states. In studies of the tightness of coupling, therefore, simple substrate-inhibitor combinations should be applied to exclude a shift in substrate competition that may occur when providing physiological substrate cocktails.
- In studies of isolated mitochondria, the mitochondrial recovery and yield should be reported. Experimental criteria such as transmission electron microscopy for evaluation of purity versus integrity should be considered. Mitochondrial markers—such as citrate synthase activity as an enzymatic matrix marker—provide a link to the tissue of origin on the basis of calculating the mitochondrial recovery, *i.e.*, the fraction of mitochondrial marker obtained from a unit mass of tissue. Total mitochondrial protein is frequently applied as a mitochondrial marker, which is restricted to isolated mitochondria.
- In studies of permeabilized cells, the viability of the cell culture or cell suspension of origin should be reported. Normalization should be evaluated for total cell count or viable cell count.
- Terms and symbols are summarized in **Table 8**. Their use will facilitate transdisciplinary communication and support further development of a consistent theory of bioenergetics and mitochondrial physiology. Technical terms related to and defined with normal words can be used as

1405 index terms in databases, support the creation of ontologies towards semantic information processing  
 1406 (MitoPedia), and help in communicating analytical findings as impactful data-driven stories.  
 1407 ‘Making data available without making it understandable may be worse than not making it available  
 1408 at all’ (National Academies of Sciences, Engineering, and Medicine 2018). Success will depend on  
 1409 taking further steps: (1) exhaustive text-mining considering Omics data and functional data; (2)  
 1410 network analysis of Omics data with bioinformatics tools; (3) cross-validation with distinct  
 1411 bioinformatics approaches; (4) correlation with functional data; (5) guidelines for biological  
 1412 validation of network data. This is a call to carefully contribute to FAIR principles (Findable,  
 1413 Accessible, Interoperable, Reusable) for the sharing of scientific data.

1415  
 1416 **Table 8. Terms, symbols, and units.**

1419 1420	Term	Symbol	Unit	Links and comments
1421	1422 alternative quinol oxidase	AOX		Figure 2B
1423	adenosine monophosphate	AMP		2 ADP ↔ ATP+AMP
1424	adenosine diphosphate	ADP		Table 1, Figures 2 and 5
1425	adenosine triphosphate	ATP		Figures 2 and 5
1426	adenylates	AMP, ADP, ATP		Section 2.5.1
1427	amount of substance B	$n_B$	[mol]	
1428	ATP yield per O <sub>2</sub>	$Y_{P_{ATP}/O_2}$		P <sub>ATP</sub> /O <sub>2</sub> ratio measured in any respiratory state
1429				
1430	catabolic reaction	k		Figures 1 and 3
1431	catabolic respiration	$J_{kO_2}$	<i>varies</i>	Figures 1 and 3
1432	cell number	$N_{ce}$	[x]	$N_{ce} = N_{vce} + N_{dce}$ ; Table 5
1433	cell respiration	$J_{rO_2}$	<i>varies</i>	Figure 1
1434	cell viability index	$VI$		$VI = N_{vce}/N_{ce} = 1 - N_{dce}/N_{ce}$
1435	charge number of entity B	$z_B$		Table 6; $z_{O_2} = 4$
1436	Complexes I to IV	CI to CIV		respiratory ET Complexes; Figure 2B
1437				
1438	concentration of substance B	$c_B = n_B \cdot V^{-1}$ ; [B]	[mol·m <sup>-3</sup> ]	Box 2
1439	coupling control state	CCS		Section 2.4.1
1440	dead cell number	$N_{dce}$	[x]	non-viable cells, loss of plasma membrane barrier function; Table 5
1441				
1442	electric format	$e$	[C]	Table 6
1443	electron transfer system	ETS		state; Figures 2B and 4
1444	ET state	ET		Table 1, Figures 2B and 4; State 3u
1445	ET-capacity	$E$	<i>varies</i>	Table 1, Figure 4
1446	flow, for substance B	$I_B$	[mol·s <sup>-1</sup> ]	system-related extensive quantity; Figure 6
1447				
1448	flux, for substance B	$J_B$	<i>varies</i>	size-specific quantity; Figure 6
1449	inorganic phosphate	P <sub>i</sub>		Figure 2C
1450	inorganic phosphate carrier	PiC		Figure 2C
1451	intact cell number,			
1452	viable cell number	$N_{vce}$	[x]	viable cells, intact plasma membrane barrier function; Table 5
1453				
1454	LEAK state	<b>LEAK</b>		state; Table 1, Figure 4; compare State 4
1455				
1456	LEAK-respiration	$L$	<i>varies</i>	Table 1; Figure 4
1457	mass format	$m$	[kg]	Table 4, Figure 6
1458	mass of sample X	$m_X$	[kg]	Table 4
1459	mass, dry mass	$m_d$	[kg]	mass of sample X; Figure 6 (frequently called dry weight)
1460				
1461	mass, wet mass	$m_w$	[kg]	mass of sample X; Figure 6 (frequently called wet weight)
1462				

1463	mass of object $X$	$M_X = m_X N_X^{-1}$	[kg·x <sup>-1</sup> ]	mass of entity $X$ ; Table 4
1464	MITOCARTA			<a href="https://www.broadinstitute.org/scientific-community/science/programs/metabolic-disease-program/publications/mitocarta/mitocarta-in-0">https://www.broadinstitute.org/scientific-community/science/programs/metabolic-disease-program/publications/mitocarta/mitocarta-in-0</a>
1465				
1466				
1467				
1468				
1469	MitoPedia			<a href="http://www.bioblast.at/index.php/MitoPedia">http://www.bioblast.at/index.php/MitoPedia</a>
1470	mitochondria or mitochondrial	mt		Box 1
1471	mitochondrial DNA	mtDNA		Box 1
1472	mitochondrial concentration	$C_{mtE} = mtE \cdot V^{-1}$	[mtEU·m <sup>-3</sup> ]	Table 4
1473	mitochondrial content	$mtE_X$	[mtEU·x <sup>-1</sup> ]	$mtE_X = mtE \cdot N_X^{-1}$ ; Table 4
1474	mitochondrial			
1475	elementary component	$mtE$	[mtEU]	quantity of mt-marker; Table 4
1476	mitochondrial elementary unit	mtEU	<i>varies</i>	specific units for mt-marker; Table 4
1477	mitochondrial inner membrane	mtIM		MIM is widely used; the first M is replaced by mt; Figure 2; Box 1
1478				
1479	mitochondrial outer membrane	mtOM		MOM is widely used; the first M is replaced by mt; Figure 2; Box 1
1480				
1481	mitochondrial recovery	$Y_{mtE}$		fraction of $mtE$ recovered in sample from the tissue of origin
1482				
1483	mitochondrial yield	$Y_{mtE/\underline{m}}$		mt-yield per tissues mass; $Y_{mtE/\underline{m}} = Y_{mtE} \cdot D_{mtE}$
1484				
1485	molar format	$\underline{n}$	[mol]	Table 6
1486	negative	neg		Figure 4
1487	number concentration of $X$	$C_{NX}$	[x·m <sup>-3</sup> ]	Table 4
1488	number format	$\underline{N}$	[x]	Table 4, Figure 6
1489	number of entities $X$	$N_X$	[x]	Table 4, Figure 6
1490	number of entity B	$N_B$	[x]	Table 4
1491	oxidative phosphorylation	<b>OXPHOS</b>		state; Table 1, Figure 4
1492	OXPHOS state	<b>OXPHOS</b>		Table 1; State 3 if [ADP] and [P <sub>i</sub> ] are saturating
1493				
1494	OXPHOS-capacity	$P$	<i>varies</i>	Table 1, Figure 4
1495	oxygen concentration	$c_{O_2} = n_{O_2} \cdot V^{-1}$	[mol·m <sup>-3</sup> ]	[O <sub>2</sub> ]; Section 3.2
1496	oxygen flux, in reaction r	$J_{rO_2}$	<i>varies</i>	Figure 1
1497	pathway control state	PCS		Section 2.2
1498	permeabilized cell number	$N_{pcc}$	[x]	experimental permeabilization of plasma membrane; Table 5
1499				
1500	phosphorylation of ADP to ATP	P $\gg$		Section 2.2
1501	P $\gg$ /O <sub>2</sub> ratio	P $\gg$ /O <sub>2</sub>		mechanistic $Y_{P\gg/O_2}$ , calculated from pump stoichiometries; Figure 2B
1502				
1503	positive	pos		Figure 4
1504	proton in the negative compartment	H <sup>+</sup> <sub>neg</sub>		Figure 4
1505	proton in the positive compartment	H <sup>+</sup> <sub>pos</sub>		Figure 4
1506	protonmotive force	pmf	[V]	Figures 1, 2A and 4; Table 1
1507	rate of electron transfer in ET state	$E$	<i>varies</i>	ET-capacity; Table 1
1508	rate of LEAK-respiration	$L$	<i>varies</i>	Table 1
1509	rate of oxidative phosphorylation	$P$	<i>varies</i>	OXPHOS-capacity; Table 1
1510	rate of residual oxygen consumption	$Rox$		Table 1, Figure 1
1511	residual oxygen consumption	ROX		state; Table 1
1512	respiratory supercomplex	SC I <sub>n</sub> III <sub>n</sub> IV <sub>n</sub>		supramolecular assemblies composed of variable copy numbers ( $n$ ) of CI, CIII and CIV; Box 1
1513				
1514				
1515	specific mitochondrial density	$D_{mtE} = mtE \cdot m_X^{-1}$	[mtEU·kg <sup>-1</sup> ]	Table 4
1516	substrate-uncoupler-inhibitor-titration protocol	SUIT		Section 2.2
1517				
1518	volume	$V$	[m <sup>-3</sup> ]	Table 7



1520  
1521  
1522 Experimentally, respiration is separated in mitochondrial preparations from the interactions with  
1523 the fermentative pathways of the intact cell. OXPHOS analysis is based on the study of mitochondrial  
1524 preparations complementary to bioenergetic investigations of intact cells and organisms—from model  
1525 organisms to the human species including healthy and diseased persons (patients). Different mechanisms  
1526 of respiratory uncoupling have to be distinguished (**Figure 3**). Metabolic fluxes measured in defined  
1527 coupling and pathway control states (**Figures 5 and 6**) provide insights into the meaning of cellular and  
1528 organismic respiration.

1529 The optimal choice for expressing mitochondrial and cell respiration as O<sub>2</sub> flow per biological  
1530 sample, and normalization for specific tissue-markers (volume, mass, protein) and mitochondrial  
1531 markers (volume, protein, content, mtDNA, activity of marker enzymes, respiratory reference state) is  
1532 guided by the scientific question under study. Interpretation of the data depends critically on appropriate  
1533 normalization (**Figure 6**).

1534 MitoEAGLE can serve as a gateway to better diagnose mitochondrial respiratory adaptations and  
1535 defects linked to genetic variation, age-related health risks, sex-specific mitochondrial performance,  
1536 lifestyle with its effects on degenerative diseases, and thermal and chemical environment. The present  
1537 recommendations on coupling control states and rates, linked to the concept of the protonmotive force,  
1538 are focused on studies using mitochondrial preparations (**Box 3**). These will be extended in a series of  
1539 reports on pathway control of mitochondrial respiration, respiratory states in intact cells, and  
1540 harmonization of experimental procedures.

#### 1541 **Acknowledgements**

1542 We thank Beno M for management assistance, and Rich PR for valuable discussions. This publication  
1543 is based upon work from COST Action CA15203 MitoEAGLE, supported by COST (European  
1544 Cooperation in Science and Technology), in cooperation with COST Actions CA16225 EU-  
1545 CARDIOPROTECTION and CA17129 CardioRNA, and K-Regio project MitoFit (E.G.).

1546  
1547  
1548 **Competing financial interests:** E.G. is founder and CEO of Oroboros Instruments, Innsbruck, Austria.  
1549

#### 1550 **References**

- 1551  
1552 Altmann R (1894) Die Elementarorganismen und ihre Beziehungen zu den Zellen. Zweite vermehrte Auflage.  
1553 Verlag Von Veit & Comp, Leipzig:160 pp.  
1554 Baggeto LG, Testa-Perussini R (1990) Role of acetoin on the regulation of intermediate metabolism of Ehrlich  
1555 ascites tumor mitochondria: its contribution to membrane cholesterol enrichment modifying passive proton  
1556 permeability. Arch Biochem Biophys 283:341-8.  
1557 Beard DA (2005) A biophysical model of the mitochondrial respiratory system and oxidative phosphorylation.  
1558 PLoS Comput Biol 1(4):e36.  
1559 Benda C (1898) Weitere Mitteilungen über die Mitochondria. Verh Dtsch Physiol Ges:376-83.  
1560 Birkedal R, Laasmaa M, Vendelin M (2014) The location of energetic compartments affects energetic  
1561 communication in cardiomyocytes. Front Physiol 5:376.  
1562 Blier PU, Dufresne F, Burton RS (2001) Natural selection and the evolution of mtDNA-encoded peptides:  
1563 evidence for intergenomic co-adaptation. Trends Genet 17:400-6.  
1564 Blier PU, Guderley HE (1993) Mitochondrial activity in rainbow trout red muscle: the effect of temperature on  
1565 the ADP-dependence of ATP synthesis. J Exp Biol 176:145-58.  
1566 Breton S, Beaupré HD, Stewart DT, Hoeh WR, Blier PU (2007) The unusual system of doubly uniparental  
1567 inheritance of mtDNA: isn't one enough? Trends Genet 23:465-74.  
1568 Brown GC (1992) Control of respiration and ATP synthesis in mammalian mitochondria and cells. Biochem J  
1569 284:1-13.  
1570 Burger G, Gray MW, Forget L, Lang BF (2013) Strikingly bacteria-like and gene-rich mitochondrial genomes  
1571 throughout jakobid protists. Genome Biol Evol 5:418-38.  
1572 Calvo SE, Klauser CR, Mootha VK (2016) MitoCarta2.0: an updated inventory of mammalian mitochondrial  
1573 proteins. Nucleic Acids Research 44:D1251-7.  
1574 Calvo SE, Julien O, Clauser KR, Shen H, Kamer KJ, Wells JA, Mootha VK (2017) Comparative analysis of  
1575 mitochondrial N-termini from mouse, human, and yeast. Mol Cell Proteomics 16:512-23.

- 1576 Campos JC, Queliconi BB, Bozi LHM, Bechara LRG, Dourado PMM, Andres AM, Jannig PR, Gomes KMS,  
 1577 Zambelli VO, Rocha-Resende C, Guatimosim S, Brum PC, Mochly-Rosen D, Gottlieb RA, Kowaltowski AJ,  
 1578 Ferreira JCB (2017) Exercise reestablishes autophagic flux and mitochondrial quality control in heart failure.  
 1579 *Autophagy* 13:1304-317.
- 1580 Canton M, Luvisetto S, Schmehl I, Azzone GF (1995) The nature of mitochondrial respiration and  
 1581 discrimination between membrane and pump properties. *Biochem J* 310:477-81.
- 1582 Carrico C, Meyer JG, He W, Gibson BW, Verdin E (2018) The mitochondrial acylome emerges: proteomics,  
 1583 regulation by Sirtuins, and metabolic and disease implications. *Cell Metab* 27:497-512.
- 1584 Chan DC (2006) Mitochondria: dynamic organelles in disease, aging, and development. *Cell* 125:1241-52.
- 1585 Chance B, Williams GR (1955a) Respiratory enzymes in oxidative phosphorylation. I. Kinetics of oxygen  
 1586 utilization. *J Biol Chem* 217:383-93.
- 1587 Chance B, Williams GR (1955b) Respiratory enzymes in oxidative phosphorylation: III. The steady state. *J Biol*  
 1588 *Chem* 217:409-27.
- 1589 Chance B, Williams GR (1955c) Respiratory enzymes in oxidative phosphorylation. IV. The respiratory chain. *J*  
 1590 *Biol Chem* 217:429-38.
- 1591 Chance B, Williams GR (1956) The respiratory chain and oxidative phosphorylation. *Adv Enzymol Relat Subj*  
 1592 *Biochem* 17:65-134.
- 1593 Chowdhury SK, Djordjevic J, Albensi B, Fernyhough P (2015) Simultaneous evaluation of substrate-dependent  
 1594 oxygen consumption rates and mitochondrial membrane potential by TMRM and safranin in cortical  
 1595 mitochondria. *Biosci Rep* 36:e00286.
- 1596 Cobb LJ, Lee C, Xiao J, Yen K, Wong RG, Nakamura HK, Mehta HH, Gao Q, Ashur C, Huffman DM, Wan J,  
 1597 Muzumdar R, Barzilai N, Cohen P (2016) Naturally occurring mitochondrial-derived peptides are age-  
 1598 dependent regulators of apoptosis, insulin sensitivity, and inflammatory markers. *Aging (Albany NY)* 8:796-  
 1599 809.
- 1600 Cohen ER, Cvitas T, Frey JG, Holmström B, Kuchitsu K, Marquardt R, Mills I, Pavese F, Quack M, Stohner J,  
 1601 Strauss HL, Takami M, Thor HL (2008) Quantities, units and symbols in physical chemistry, IUPAC Green  
 1602 Book, 3rd Edition, 2nd Printing, IUPAC & RSC Publishing, Cambridge.
- 1603 Cooper H, Hedges LV, Valentine JC, eds (2009) *The handbook of research synthesis and meta-analysis*. Russell  
 1604 Sage Foundation.
- 1605 Coopersmith J (2010) Energy, the subtle concept. The discovery of Feynman's blocks from Leibnitz to Einstein.  
 1606 Oxford University Press:400 pp.
- 1607 Cummins J (1998) Mitochondrial DNA in mammalian reproduction. *Rev Reprod* 3:172-82.
- 1608 Dai Q, Shah AA, Garde RV, Yonish BA, Zhang L, Medvitz NA, Miller SE, Hansen EL, Dunn CN, Price TM  
 1609 (2013) A truncated progesterone receptor (PR-M) localizes to the mitochondrion and controls cellular  
 1610 respiration. *Mol Endocrinol* 27:741-53.
- 1611 Daum B, Walter A, Horst A, Osiewacz HD, Kühlbrandt W (2013) Age-dependent dissociation of ATP synthase  
 1612 dimers and loss of inner-membrane cristae in mitochondria. *Proc Natl Acad Sci U S A* 110:15301-6.
- 1613 Divakaruni AS, Brand MD (2011) The regulation and physiology of mitochondrial proton leak. *Physiology*  
 1614 (Bethesda) 26:192-205.
- 1615 Doerrier C, Garcia-Souza LF, Krumschnabel G, Wohlfarter Y, Mészáros AT, Gnaiger E (2018) High-Resolution  
 1616 FluoRespirometry and OXPHOS protocols for human cells, permeabilized fibres from small biopsies of  
 1617 muscle, and isolated mitochondria. *Methods Mol Biol* 1782 (Palmeira CM, Moreno AJ, eds): Mitochondrial  
 1618 Bioenergetics, 978-1-4939-7830-4.
- 1619 Doskey CM, van 't Erve TJ, Wagner BA, Buettner GR (2015) Moles of a substance per cell is a highly  
 1620 informative dosing metric in cell culture. *PLoS One* 10:e0132572.
- 1621 Drahotová Z, Milerová M, Stieglerová A, Houstek J, Ostádal B (2004) Developmental changes of cytochrome *c*  
 1622 oxidase and citrate synthase in rat heart homogenate. *Physiol Res* 53:119-22.
- 1623 Duarte FV, Palmeira CM, Rolo AP (2014) The role of microRNAs in mitochondria: small players acting wide.  
 1624 *Genes (Basel)* 5:865-86.
- 1625 Ehinger JK, Morota S, Hansson MJ, Paul G, Elmér E (2015) Mitochondrial dysfunction in blood cells from  
 1626 amyotrophic lateral sclerosis patients. *J Neurol* 262:1493-503.
- 1627 Ernster L, Schatz G (1981) Mitochondria: a historical review. *J Cell Biol* 91:227s-55s.
- 1628 Estabrook RW (1967) Mitochondrial respiratory control and the polarographic measurement of ADP:O ratios.  
 1629 *Methods Enzymol* 10:41-7.
- 1630 Faber C, Zhu ZJ, Castellino S, Wagner DS, Brown RH, Peterson RA, Gates L, Barton J, Bickett M, Hagerty L,  
 1631 Kimbrough C, Sola M, Bailey D, Jordan H, Elangbam CS (2014) Cardiolipin profiles as a potential  
 1632 biomarker of mitochondrial health in diet-induced obese mice subjected to exercise, diet-restriction and  
 1633 ephedrine treatment. *J Appl Toxicol* 34:1122-9.
- 1634 Feagin JE, Harrell MI, Lee JC, Coe KJ, Sands BH, Cannone JJ, Tami G, Schnare MN, Gutell RR (2012) The  
 1635 fragmented mitochondrial ribosomal RNAs of *Plasmodium falciparum*. *PLoS One* 7:e38320.
- 1636 Fell D (1997) *Understanding the control of metabolism*. Portland Press.

- 1637 Forstner H, Gnaiger E (1983) Calculation of equilibrium oxygen concentration. In: Polarographic Oxygen  
1638 Sensors. Aquatic and Physiological Applications. Gnaiger E, Forstner H (eds), Springer, Berlin, Heidelberg,  
1639 New York:321-33.
- 1640 Garlid KD, Beavis AD, Ratkje SK (1989) On the nature of ion leaks in energy-transducing membranes. *Biochim*  
1641 *Biophys Acta* 976:109-20.
- 1642 Garlid KD, Semrad C, Zinchenko V. Does redox slip contribute significantly to mitochondrial respiration? In:  
1643 Schuster S, Rigoulet M, Ouhabi R, Mazat J-P, eds (1993) *Modern trends in biothermokinetics*. Plenum Press,  
1644 New York, London:287-93.
- 1645 Gerö D, Szabo C (2016) Glucocorticoids suppress mitochondrial oxidant production via upregulation of  
1646 uncoupling protein 2 in hyperglycemic endothelial cells. *PLoS One* 11:e0154813.
- 1647 Gnaiger E. Efficiency and power strategies under hypoxia. Is low efficiency at high glycolytic ATP production a  
1648 paradox? In: *Surviving Hypoxia: Mechanisms of Control and Adaptation*. Hochachka PW, Lutz PL, Sick T,  
1649 Rosenthal M, Van den Thillart G, eds (1993a) CRC Press, Boca Raton, Ann Arbor, London, Tokyo:77-109.
- 1650 Gnaiger E (1993b) Nonequilibrium thermodynamics of energy transformations. *Pure Appl Chem* 65:1983-2002.
- 1651 Gnaiger E (2001) Bioenergetics at low oxygen: dependence of respiration and phosphorylation on oxygen and  
1652 adenosine diphosphate supply. *Respir Physiol* 128:277-97.
- 1653 Gnaiger E (2009) Capacity of oxidative phosphorylation in human skeletal muscle. New perspectives of  
1654 mitochondrial physiology. *Int J Biochem Cell Biol* 41:1837-45.
- 1655 Gnaiger E (2014) Mitochondrial pathways and respiratory control. An introduction to OXPHOS analysis. 4th ed.  
1656 *Mitochondr Physiol Network* 19.12. Oroboros MiPNet Publications, Innsbruck:80 pp.
- 1657 Gnaiger E, Méndez G, Hand SC (2000) High phosphorylation efficiency and depression of uncoupled respiration  
1658 in mitochondria under hypoxia. *Proc Natl Acad Sci USA* 97:11080-5.
- 1659 Greggio C, Jha P, Kulkarni SS, Lagarrigue S, Broskey NT, Boutant M, Wang X, Conde Alonso S, Ofori E,  
1660 Auwerx J, Cantó C, Amati F (2017) Enhanced respiratory chain supercomplex formation in response to  
1661 exercise in human skeletal muscle. *Cell Metab* 25:301-11.
- 1662 Hinkle PC (2005) P/O ratios of mitochondrial oxidative phosphorylation. *Biochim Biophys Acta* 1706:1-11.
- 1663 Hofstadter DR (1979) Gödel, Escher, Bach: An eternal golden braid. A metaphorical fugue on minds and  
1664 machines in the spirit of Lewis Carroll. Harvester Press:499 pp.
- 1665 Illaste A, Laasmaa M, Peterson P, Vendelin M (2012) Analysis of molecular movement reveals latticelike  
1666 obstructions to diffusion in heart muscle cells. *Biophys J* 102:739-48.
- 1667 Jasienski M, Bazzaz FA (1999) The fallacy of ratios and the testability of models in biology. *Oikos* 84:321-26.
- 1668 Jepihhina N, Beraud N, Sepp M, Birkedal R, Vendelin M (2011) Permeabilized rat cardiomyocyte response  
1669 demonstrates intracellular origin of diffusion obstacles. *Biophys J* 101:2112-21.
- 1670 Karnkowska A, Vacek V, Zubáčová Z, Treitli SC, Petrželková R, Eme L, Novák L, Žárský V, Barlow LD,  
1671 Herman EK, Soukal P, Hroudová M, Doležal P, Stairs CW, Roger AJ, Eliáš M, Dacks JB, Vlček Č, Hampl V  
1672 (2016) A eukaryote without a mitochondrial organelle. *Curr Biol* 26:1274-84.
- 1673 Klepinin A, Ounpuu L, Guzun R, Chekulayev V, Timohhina N, Tepp K, Shevchuk I, Schlattner U, Kaambre T  
1674 (2016) Simple oxygraphic analysis for the presence of adenylate kinase 1 and 2 in normal and tumor cells. *J*  
1675 *Bioenerg Biomembr* 48:531-48.
- 1676 Klingenberg M (2017) UCP1 - A sophisticated energy valve. *Biochimie* 134:19-27.
- 1677 Koit A, Shevchuk I, Ounpuu L, Klepinin A, Chekulayev V, Timohhina N, Tepp K, Puurand M, Truu L, Heck K,  
1678 Valvere V, Guzun R, Kaambre T (2017) Mitochondrial respiration in human colorectal and breast cancer  
1679 clinical material is regulated differently. *Oxid Med Cell Longev* 1372640.
- 1680 Komlódi T, Tretter L (2017) Methylene blue stimulates substrate-level phosphorylation catalysed by succinyl-  
1681 CoA ligase in the citric acid cycle. *Neuropharmacology* 123:287-98.
- 1682 Korn E (1969) Cell membranes: structure and synthesis. *Annu Rev Biochem* 38:263-88.
- 1683 Lai N, M Kummitha C, Rosca MG, Fujioka H, Tandler B, Hoppel CL (2018) Isolation of mitochondrial  
1684 subpopulations from skeletal muscle: optimizing recovery and preserving integrity. *Acta Physiol*  
1685 (Oxf):e13182. doi: 10.1111/apha.13182.
- 1686 Lane N (2005) *Power, sex, suicide: mitochondria and the meaning of life*. Oxford University Press:354 pp.
- 1687 Larsen S, Nielsen J, Neigaard Nielsen C, Nielsen LB, Wibrand F, Stride N, Schroder HD, Boushel RC, Helge  
1688 JW, Dela F, Hey-Mogensen M (2012) Biomarkers of mitochondrial content in skeletal muscle of healthy  
1689 young human subjects. *J Physiol* 590:3349-60.
- 1690 Lee C, Zeng J, Drew BG, Sallam T, Martin-Montalvo A, Wan J, Kim SJ, Mehta H, Hevener AL, de Cabo R,  
1691 Cohen P (2015) The mitochondrial-derived peptide MOTS-c promotes metabolic homeostasis and reduces  
1692 obesity and insulin resistance. *Cell Metab* 21:443-54.
- 1693 Lee SR, Kim HK, Song IS, Youm J, Dizon LA, Jeong SH, Ko TH, Heo HJ, Ko KS, Rhee BD, Kim N, Han J  
1694 (2013) Glucocorticoids and their receptors: insights into specific roles in mitochondria. *Prog Biophys Mol*  
1695 *Biol* 112:44-54.
- 1696 Leek BT, Mudaliar SR, Henry R, Mathieu-Costello O, Richardson RS (2001) Effect of acute exercise on citrate  
1697 synthase activity in untrained and trained human skeletal muscle. *Am J Physiol Regul Integr Comp Physiol*  
1698 280:R441-7.

- 1699 Lemieux H, Blier PU, Gnaiger E (2017) Remodeling pathway control of mitochondrial respiratory capacity by  
1700 temperature in mouse heart: electron flow through the Q-junction in permeabilized fibers. *Sci Rep* 7:2840.
- 1701 Lenaz G, Tioli G, Falasca AI, Genova ML (2017) Respiratory supercomplexes in mitochondria. In: *Mechanisms*  
1702 *of primary energy trasduction in biology*. M Wikstrom (ed) Royal Society of Chemistry Publishing, London,  
1703 UK:296-337.
- 1704 Liu S, Roellig DM, Guo Y, Li N, Frace MA, Tang K, Zhang L, Feng Y, Xiao L (2016) Evolution of mitosome  
1705 metabolism and invasion-related proteins in *Cryptosporidium*. *BMC Genomics* 17:1006.
- 1706 Margulis L (1970) *Origin of eukaryotic cells*. New Haven: Yale University Press.
- 1707 McDonald AE, Vanlerberghe GC, Staples JF (2009) Alternative oxidase in animals: unique characteristics and  
1708 taxonomic distribution. *J Exp Biol* 212:2627-34.
- 1709 Meinild Lundby AK, Jacobs RA, Gehrig S, de Leur J, Hauser M, Bonne TC, Flück D, Dandanell S, Kirk N,  
1710 Kaech A, Ziegler U, Larsen S, Lundby C (2018) Exercise training increases skeletal muscle mitochondrial  
1711 volume density by enlargement of existing mitochondria and not de novo biogenesis. *Acta Physiol* 222,  
1712 e12905.
- 1713 Menshikova EV, Ritov VB, Fairfull L, Ferrell RE, Kelley DE, Goodpaster BH (2006) Effects of exercise on  
1714 mitochondrial content and function in aging human skeletal muscle. *J Gerontol A Biol Sci Med Sci* 61:534-  
1715 40.
- 1716 Menshikova EV, Ritov VB, Ferrell RE, Azuma K, Goodpaster BH, Kelley DE (2007) Characteristics of skeletal  
1717 muscle mitochondrial biogenesis induced by moderate-intensity exercise and weight loss in obesity. *J Appl*  
1718 *Physiol* (1985) 103:21-7.
- 1719 Menshikova EV, Ritov VB, Toledo FG, Ferrell RE, Goodpaster BH, Kelley DE (2005) Effects of weight loss  
1720 and physical activity on skeletal muscle mitochondrial function in obesity. *Am J Physiol Endocrinol Metab*  
1721 288:E818-25.
- 1722 Miller GA (1991) *The science of words*. Scientific American Library New York:276 pp.
- 1723 Mitchell P (1961) Coupling of phosphorylation to electron and hydrogen transfer by a chemi-osmotic type of  
1724 mechanism. *Nature* 191:144-8.
- 1725 Mitchell P (2011) Chemiosmotic coupling in oxidative and photosynthetic phosphorylation. *Biochim Biophys*  
1726 *Acta Bioenergetics* 1807:1507-38.
- 1727 Mogensen M, Sahlin K, Fernström M, Glinthborg D, Vind BF, Beck-Nielsen H, Højlund K (2007) Mitochondrial  
1728 respiration is decreased in skeletal muscle of patients with type 2 diabetes. *Diabetes* 56:1592-9.
- 1729 Mohr PJ, Phillips WD (2015) Dimensionless units in the SI. *Metrologia* 52:40-7.
- 1730 Moreno M, Giacco A, Di Munno C, Goglia F (2017) Direct and rapid effects of 3,5-diiodo-L-thyronine (T2).  
1731 *Mol Cell Endocrinol* 7207:30092-8.
- 1732 Morrow RM, Picard M, Derbeneva O, Leipzig J, McManus MJ, Gouspillou G, Barbat-Artigas S, Dos Santos C,  
1733 Hepple RT, Murdock DG, Wallace DC (2017) Mitochondrial energy deficiency leads to hyperproliferation of  
1734 skeletal muscle mitochondria and enhanced insulin sensitivity. *Proc Natl Acad Sci U S A* 114:2705-10.
- 1735 Murley A, Nunnari J (2016) The emerging network of mitochondria-organelle contacts. *Mol Cell* 61:648-53.
- 1736 National Academies of Sciences, Engineering, and Medicine (2018) *International coordination for science data*  
1737 *infrastructure: Proceedings of a workshop—in brief*. Washington, DC: The National Academies Press. doi:  
1738 <https://doi.org/10.17226/25015>.
- 1739 Oemer G, Lackner L, Muigg K, Krumschnabel G, Watschinger K, Sailer S, Lindner H, Gnaiger E, Wortmann  
1740 SB, Werner ER, Zschocke J, Keller MA (2018) The molecular structural diversity of mitochondrial  
1741 cardiolipins. *Proc Nat Acad Sci U S A* 115:4158-63.
- 1742 Palmfeldt J, Bross P (2017) Proteomics of human mitochondria. *Mitochondrion* 33:2-14.
- 1743 Paradies G, Paradies V, De Benedictis V, Ruggiero FM, Petrosillo G (2014) Functional role of cardiolipin in  
1744 mitochondrial bioenergetics. *Biochim Biophys Acta* 1837:408-17.
- 1745 Pesta D, Gnaiger E (2012) High-Resolution Respirometry. *OXPHOS protocols for human cells and*  
1746 *permeabilized fibres from small biopsies of human muscle*. *Methods Mol Biol* 810:25-58.
- 1747 Pesta D, Hoppel F, Macek C, Messner H, Faulhaber M, Kobel C, Parson W, Burtcher M, Schocke M, Gnaiger  
1748 E (2011) Similar qualitative and quantitative changes of mitochondrial respiration following strength and  
1749 endurance training in normoxia and hypoxia in sedentary humans. *Am J Physiol Regul Integr Comp Physiol*  
1750 301:R1078–87.
- 1751 Price TM, Dai Q (2015) The role of a mitochondrial progesterone receptor (PR-M) in progesterone action.  
1752 *Semin Reprod Med* 33:185-94.
- 1753 Puchowicz MA, Varnes ME, Cohen BH, Friedman NR, Kerr DS, Hoppel CL (2004) Oxidative phosphorylation  
1754 analysis: assessing the integrated functional activity of human skeletal muscle mitochondria – case studies.  
1755 *Mitochondrion* 4:377-85. Puntschart A, Claassen H, Jostarndt K, Hoppeler H, Billeter R (1995) mRNAs of  
1756 enzymes involved in energy metabolism and mtDNA are increased in endurance-trained athletes. *Am J*  
1757 *Physiol* 269:C619-25.
- 1758 Quiros PM, Mottis A, Auwerx J (2016) Mitonuclear communication in homeostasis and stress. *Nat Rev Mol*  
1759 *Cell Biol* 17:213-26.



- 1760 Rackham O, Mercer TR, Filipovska A (2012) The human mitochondrial transcriptome and the RNA-binding  
1761 proteins that regulate its expression. *WIREs RNA* 3:675–95.
- 1762 Reichmann H, Hoppeler H, Mathieu-Costello O, von Bergen F, Pette D (1985) Biochemical and ultrastructural  
1763 changes of skeletal muscle mitochondria after chronic electrical stimulation in rabbits. *Pflugers Arch* 404:1-  
1764 9.
- 1765 Renner K, Amberger A, Konwalinka G, Gnaiger E (2003) Changes of mitochondrial respiration, mitochondrial  
1766 content and cell size after induction of apoptosis in leukemia cells. *Biochim Biophys Acta* 1642:115-23.
- 1767 Rice DW, Alverson AJ, Richardson AO, Young GJ, Sanchez-Puerta MV, Munzinger J, Barry K, Boore JL,  
1768 Zhang Y, dePamphilis CW, Knox EB, Palmer JD (2016) Horizontal transfer of entire genomes via  
1769 mitochondrial fusion in the angiosperm *Amborella*. *Science* 342:1468-73.
- 1770 Rich P (2003) Chemiosmotic coupling: The cost of living. *Nature* 421:583.
- 1771 Rich PR (2013) Chemiosmotic theory. *Encyclopedia Biol Chem* 1:467-72.
- 1772 Roger JA, Munoz-Gomes SA, Kamikawa R (2017) The origin and diversification of mitochondria. *Curr Biol*  
1773 27:R1177-92.
- 1774 Rostovtseva TK, Sheldon KL, Hassanzadeh E, Monge C, Saks V, Bezrukov SM, Sackett DL (2008) Tubulin  
1775 binding blocks mitochondrial voltage-dependent anion channel and regulates respiration. *Proc Natl Acad Sci*  
1776 USA 105:18746-51.
- 1777 Rustin P, Parfait B, Chretien D, Bourgeron T, Djouadi F, Bastin J, Rötig A, Munnich A (1996) Fluxes of  
1778 nicotinamide adenine dinucleotides through mitochondrial membranes in human cultured cells. *J Biol Chem*  
1779 271:14785-90.
- 1780 Saks VA, Veksler VI, Kuznetsov AV, Kay L, Sikk P, Tiivel T, Tranqui L, Olivares J, Winkler K, Wiedemann F,  
1781 Kunz WS (1998) Permeabilised cell and skinned fiber techniques in studies of mitochondrial function in  
1782 vivo. *Mol Cell Biochem* 184:81-100.
- 1783 Salabei JK, Gibb AA, Hill BG (2014) Comprehensive measurement of respiratory activity in permeabilized cells  
1784 using extracellular flux analysis. *Nat Protoc* 9:421-38.
- 1785 Sazanov LA (2015) A giant molecular proton pump: structure and mechanism of respiratory complex I. *Nat Rev*  
1786 *Mol Cell Biol* 16:375-88.
- 1787 Schneider TD (2006) Claude Shannon: biologist. The founder of information theory used biology to formulate  
1788 the channel capacity. *IEEE Eng Med Biol Mag* 25:30-3.
- 1789 Schönfeld P, Dymkowska D, Wojtczak L (2009) Acyl-CoA-induced generation of reactive oxygen species in  
1790 mitochondrial preparations is due to the presence of peroxisomes. *Free Radic Biol Med* 47:503-9.
- 1791 Schultz J, Wiesner RJ (2000) Proliferation of mitochondria in chronically stimulated rabbit skeletal muscle--  
1792 transcription of mitochondrial genes and copy number of mitochondrial DNA. *J Bioenerg Biomembr* 32:627-  
1793 34.
- 1794 Speijer D (2016) Being right on Q: shaping eukaryotic evolution. *Biochem J* 473:4103-27.
- 1795 Sugiura A, Mattie S, Prudent J, McBride HM (2017) Newly born peroxisomes are a hybrid of mitochondrial and  
1796 ER-derived pre-peroxisomes. *Nature* 542:251-4.
- 1797 Simson P, Jephthina N, Laasmaa M, Peterson P, Birkedal R, Vendelin M (2016) Restricted ADP movement in  
1798 cardiomyocytes: Cytosolic diffusion obstacles are complemented with a small number of open mitochondrial  
1799 voltage-dependent anion channels. *J Mol Cell Cardiol* 97:197-203.
- 1800 Stucki JW, Ineichen EA (1974) Energy dissipation by calcium recycling and the efficiency of calcium transport  
1801 in rat-liver mitochondria. *Eur J Biochem* 48:365-75.
- 1802 Tonkonogi M, Harris B, Sahlin K (1997) Increased activity of citrate synthase in human skeletal muscle after a  
1803 single bout of prolonged exercise. *Acta Physiol Scand* 161:435-6.
- 1804 Torralba D, Baixauli F, Sánchez-Madrid F (2016) Mitochondria know no boundaries: mechanisms and functions  
1805 of intercellular mitochondrial transfer. *Front Cell Dev Biol* 4:107. eCollection 2016.
- 1806 Vamecq J, Schepers L, Parmentier G, Mannaerts GP (1987) Inhibition of peroxisomal fatty acyl-CoA oxidase by  
1807 antimycin A. *Biochem J* 248:603-7.
- 1808 Waczulikova I, Habodaszova D, Cagalinec M, Ferko M, Ulicna O, Mateasik A, Sikurova L, Ziegelhöffer A  
1809 (2007) Mitochondrial membrane fluidity, potential, and calcium transients in the myocardium from acute  
1810 diabetic rats. *Can J Physiol Pharmacol* 85:372-81.
- 1811 Wagner BA, Venkataraman S, Buettner GR (2011) The rate of oxygen utilization by cells. *Free Radic Biol Med*  
1812 51:700-712.
- 1813 Wang H, Hiatt WR, Barstow TJ, Brass EP (1999) Relationships between muscle mitochondrial DNA content,  
1814 mitochondrial enzyme activity and oxidative capacity in man: alterations with disease. *Eur J Appl Physiol*  
1815 *Occup Physiol* 80:22-7.
- 1816 Watt IN, Montgomery MG, Runswick MJ, Leslie AG, Walker JE (2010) Bioenergetic cost of making an  
1817 adenosine triphosphate molecule in animal mitochondria. *Proc Natl Acad Sci U S A* 107:16823-7.
- 1818 Weibel ER, Hoppeler H (2005) Exercise-induced maximal metabolic rate scales with muscle aerobic capacity. *J*  
1819 *Exp Biol* 208:1635–44.
- 1820 White DJ, Wolff JN, Pierson M, Gemmell NJ (2008) Revealing the hidden complexities of mtDNA inheritance.  
1821 *Mol Ecol* 17:4925–42.

- 1822 Wikström M, Hummer G (2012) Stoichiometry of proton translocation by respiratory complex I and its  
 1823 mechanistic implications. *Proc Natl Acad Sci U S A* 109:4431-6.  
 1824 Williams EG, Wu Y, Jha P, Dubuis S, Blattmann P, Argmann CA, Houten SM, Amariuta T, Wolski W,  
 1825 Zamboni N, Aebersold R, Auwerx J (2016) Systems proteomics of liver mitochondria function. *Science* 352  
 1826 (6291):aad0189  
 1827 Willis WT, Jackman MR, Messer JI, Kuzmiak-Glancy S, Glancy B (2016) A simple hydraulic analog model of  
 1828 oxidative phosphorylation. *Med Sci Sports Exerc* 48:990-1000.  
 1829 Zíková A, Hampl V, Paris Z, Týč J, Lukeš J (2016) Aerobic mitochondria of parasitic protists: diverse genomes  
 1830 and complex functions. *Mol Biochem Parasitol* 209:46-57.  
 1831  
 1832

## 1833 Supplement

### 1834 S1. Manuscript phases and versions - an open-access approach

1835 This manuscript on ‘Mitochondrial respiratory states and rates’ is a position statement in the frame of COST Action  
 1836 CA15203 MitoEAGLE. The global MitoEAGLE network made it possible to collaborate with a large number of  
 1837 coauthors to reach consensus on the present manuscript. Nevertheless, we do not consider scientific progress to be  
 1838 supported by ‘declaration’ statements (other than on ethical or political issues). Our manuscript aims at providing  
 1839 arguments for further debate rather than pushing opinions. We hope to initiate a much broader process of  
 1840 discussion and want to raise the awareness of the importance of a consistent terminology for reporting of scientific  
 1841 data in the field of bioenergetics, mitochondrial physiology and pathology. Quality of research requires quality of  
 1842 communication. Some established researchers in the field may not want to re-consider the use of jargon which has  
 1843 become established despite deficiencies of accuracy and meaning. In the long run, superior standards will become  
 1844 accepted. We hope to contribute to this evolutionary process, with an emphasis on harmonization rather than  
 1845 standardization.

1846 *Phase 1* The protonmotive force and respiratory control

1847 [http://www.mitoeagle.org/index.php/The\\_protonmotive\\_force\\_and\\_respiratory\\_control](http://www.mitoeagle.org/index.php/The_protonmotive_force_and_respiratory_control)

- 1848 • 2017-04-09 to 2017-09-18 (44 versions)
- 1849 • 2017-09-21 to 2018-02-06 (44+21 versions)

1850 [http://www.mitoeagle.org/index.php/MitoEAGLE\\_preprint\\_2017-09-21](http://www.mitoeagle.org/index.php/MitoEAGLE_preprint_2017-09-21)

1851 2017-11-11: Print version (16) for MiP2017/MitoEAGLE conference in Hradec Kralove

1852 *Phase 2* Mitochondrial respiratory states and rates: Building blocks of mitochondrial physiology Part 1

1853 [http://www.mitoeagle.org/index.php/MitoEAGLE\\_preprint\\_2018-02-08](http://www.mitoeagle.org/index.php/MitoEAGLE_preprint_2018-02-08)

- 1854 • 2018-02-08 – (44+49 Versions up to 2018-12-01)

1855 *Phase 3* Mitochondrial respiratory states and rates. Submission to a preprint server: [BioRxiv](https://www.biorxiv.org/)

1856 *Phase 4* Journal submission: CELL METABOLISM, aiming at indexing by *The Web of Science* and *PubMed*.

### 1860 S2. Authors

1861 This manuscript developed as an open invitation to scientists and students to join as coauthors in the bottom-up  
 1862 spirit of COST, to provide a balanced view of mitochondrial respiratory control and a consensus statement on  
 1863 reporting data of mitochondrial respiration in terms of metabolic flows and fluxes.

1864 Coauthors are added in alphabetical order based upon a first draft written by the corresponding author, who  
 1865 edited all versions. *Coauthors confirm that they have read the final manuscript, possibly have made additions or*  
 1866 *suggestions for improvement, and agree to implement the recommendations into future manuscripts, presentations*  
 1867 *and teaching materials.*

1868 We continue to invite comments and suggestions, particularly if you are an early career investigator adding  
 1869 an open future-oriented perspective, or an established scientist providing a balanced historical basis. Your critical  
 1870 input into the quality of the manuscript will be most welcome, improving our aims to be educational, general,  
 1871 consensus-oriented, and in practice be helpful to students working in mitochondrial respiratory physiology.

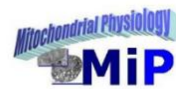
1872 To join as a coauthor, please feel free to focus on a particular section, providing direct input and references,  
 1873 and contributing to the scope of the manuscript from the perspective of your expertise. Your comments will be  
 1874 considered as appropriate in the manuscript and will be largely posted on the discussion page of the MitoEAGLE  
 1875 preprint website.  
 1876  
 1877

### 1878 S3. Joining COST Actions

- 1879 • CA15203 MitoEAGLE - [http://www.cost.eu/COST\\_Actions/ca/CA15203](http://www.cost.eu/COST_Actions/ca/CA15203)
- 1880 • CA16225 EU-CARDIOPROTECTION - [http://www.cost.eu/COST\\_Actions/ca/CA16225](http://www.cost.eu/COST_Actions/ca/CA16225)
- 1881 • CA17129 CardioRNA - [http://www.cost.eu/COST\\_Actions/ca/CA17129](http://www.cost.eu/COST_Actions/ca/CA17129)



# Mitochondrial respiratory states and rates:



## Building blocks of mitochondrial physiology

Part 1 - [www.mitoeagle.org/index.php/MitoEAGLE\\_preprint\\_2018-02-08](http://www.mitoeagle.org/index.php/MitoEAGLE_preprint_2018-02-08)

Gnaiger E<sup>1,2</sup>, corresponding author  
355 co-authors, MitoEAGLE Working Group

<sup>1</sup>Medical University Innsbruck  
<sup>2</sup>Oroboros, Innsbruck, Austria

**Aims** Clarity of concept and consistency of nomenclature facilitate effective transdisciplinary communication, education, and ultimately further discovery.

Adhering to uniform standards and harmonizing the terminology concerning mitochondrial respiratory states and rates will support the development of databases of mitochondrial respiratory function in cells, tissues, and species.

**Summary** Recommendations on coupling control states and rates are focused on studies with mitochondrial preparations.

**Fig. 1:** Respiration is defined by O<sub>2</sub> flux balance.  
**Fig. 2:** OXPHOS analysis is based on the study of mt- preparations. Metabolic fluxes measured in defined coupling and pathway control states provide insights into the meaning of cellular respiration.  
**Fig. 3:** Interpretation of respiratory rates depends critically on appropriate normalization.

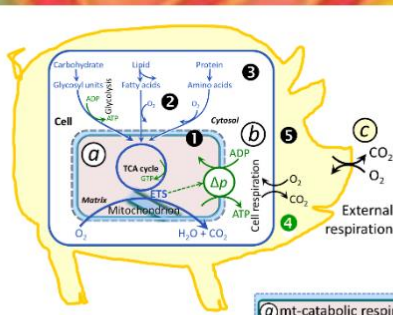
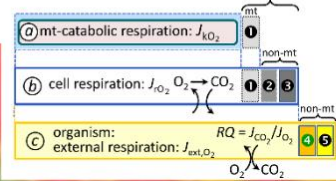


**Figure 1. From mitochondrial to external respiration**

Mitochondrial (mt) respiration is the oxidation of fuel substrates (electron donors) and reduction of O<sub>2</sub> catalysed by the electron transfer system, ETS:

- a** mt-catabolic respiration, excluding
- 1** mt-residual oxygen consumption, *Rox*.
- b** Total cellular O<sub>2</sub> consumption, including mt-*Rox*, **e** non-mt catabolic *Rox*, particularly by peroxisomal oxidases, and **e** non-mt *Rox* unrelated to catabolism.
- c** External respiration, including **1** aerobic microbial respiration, and **e** extracellular O<sub>2</sub> consumption.



MIPart by Odra Noel

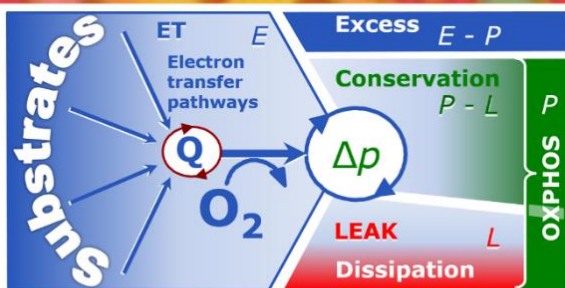


**Figure 2. Respiratory states (ET, OXPHOS, LEAK) and corresponding rates (E, P, L)**

Table 1. Coupling states and residual oxygen consumption in mitochondrial preparations in relation to respiration- and phosphorylation-flux,  $J_{kO_2}$  and  $J_{pO_2}$ , and protonmotive force,  $\Delta p$ . Coupling states are established at kinetically-saturating concentrations of fuel substrates and O<sub>2</sub>.

State	$J_{kO_2}$	$J_{pO_2}$	$\Delta p$	Inducing factors	Limiting factors
LEAK	$L$ ; low, cation leak-dependent respiration	0	max.	proton leak, slip, and cation cycling	$J_{pO_2} = 0$ : (1) without ADP, $L_{SC}$ ; (2) max. ATP/ADP ratio, $L_r$ ; or (3) inhibition of the phosphorylation-pathway, $L_{Oxy}$
OXPHOS	$P$ ; high, ADP-stimulated respiration	max.	high	kinetically-saturating [ADP] and [P <sub>i</sub> ]	$J_{kO_2}$ by phosphorylation-pathway; or $J_{kO_2}$ by ET-capacity
ET	$E$ ; max., noncoupled respiration	0	low	optimal external uncoupler concentration for max. $J_{O_{2,E}}$	$J_{kO_2}$ by ET-capacity
ROX	$Rox$ ; min., residual O <sub>2</sub> consumption	0	0	$J_{O_{2,Rox}}$ in non-ET-pathway oxidation reactions	inhibition of all ET-pathways; or absence of fuel substrates

**Figure 3. Normalization of rate**

**A:** Cell respiration is normalized for (1) the experimental **Sample** (flow per object, mass-specific flux, or cell-volume-specific flux); or (2) for methodological reasons for the **Chamber** volume.

**B:** Flow per cell [amol O<sub>2</sub> s<sup>-1</sup> cell<sup>-1</sup>] is flux per chamber volume,  $J_V$  [nmol O<sub>2</sub> s<sup>-1</sup> L<sup>-1</sup>], divided by cell concentration in the chamber,  $N_{ce}/V$  [cells L<sup>-1</sup>], which is **Number** analysis. In **Structure** analysis, aerobic cell performance is mt-quality (mt-specific flux, e.g., per citrate synthase, CS) times mt-quantity, or mt-function times mt-structure.



# COST Action CA15203 MitoEAGLE

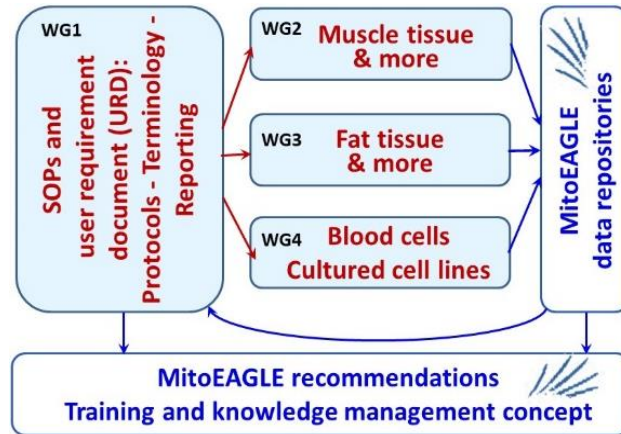
Evolution Age Gender  
Lifestyle Environment



## Mission of the global MitoEAGLE network

in collaboration with the Mitochondrial Physiology Society, MiPs

- Improve our knowledge on mitochondrial function in health and disease with regard to Evolution, Age, Gender, Lifestyle and Environment
- Interrelate studies across laboratories with the help of a MitoEAGLE data management system
- Provide standardized measures to link mitochondrial and physiological performance to understand the myriad of factors that play a role in mitochondrial physiology



Join the COST Action MitoEAGLE - contribute to the quality management network.



More information:  
[www.mitoeagle.org](http://www.mitoeagle.org)



Funded by the Horizon 2020 Framework Programme  
of the European Union

